2 Chapter two

Risks from a rapidly changing climate

The observations that anthropogenic CO_2 emissions and sea level are rising at rates at or near the upper levels of IPCC projections have raised concerns about the risks posed by rapid climate change. Although some analyses of the potential impacts of high-end projections have been made, much research on climate change impacts to date has tended to focus more strongly on the mid range values of the IPCC projections, and have naturally tended to place less weight on outliers when a range of scenarios is considered. In this section several of the risks associated with observed and projected rates of climate change are explored in more detail, including sea-level rise, drought and drying, ocean acidification and extreme events.

… much research on climate change impacts to date has tended to focus more strongly on the mid range values of the IPCC projections

2.1 Melting ice and rising sea level

Sea-level rise has emerged as one of the most intensely debated issues in the scientific community following the publication of the IPCC's AR4. Some of the debate has arisen because of confusion about the interpretation of the AR4's sea-level rise projections, which have been erroneously interpreted in some quarters as lowering the upper limit of the projections compared to those of the IPCC's Third Assessment Report in 2001.

The confusion has arisen because of the way in which the contributions to sea-level rise from the large polar ice sheets have been treated in the assessments. In the Third Assessment Report an estimate was made of potential contributions from the dynamics of polar ice sheets and included in the projections to 2100 (Figure 3), leading to a range of 0.11 to 0.88 m. In the AR4, however, estimates of the contributions from polar ice sheet dynamics, because they cannot yet be modelled quantitatively with confidence, were excluded from the projections, leading to an apparently narrower range of 0.18 to 0.59 m (Figure 3). When estimates from the AR4 of contributions from polar ice sheet dynamics are included (–0.01 to 0.17 m – see final row of Table 10.7 of the AR4 Working Group I Report), the range of AR4 projections becomes 0.18 to 0.76 m (Figure 3), which is not significantly different from projections in the Third Assessment Report. The IPCC noted that higher sea-level rises could not be ruled out.

Progress has been made since the AR4 in quantifying the individual factors that contribute to sea-level rise. The contributions from small glaciers can now be better represented by geodetic and direct mass–balance measurements; the estimated contribution is 1.1–1.4 mm yr^{-1} for the period 2001–05 (Cogley 2009); these contributions may increase through the 21st century (Meier et al. 2007). Improved estimates of heat content for the upper 300 m and 700 m of the ocean show that warming and thermal expansion trends for the period 1961–2003 are about 50% larger than earlier estimates. When the improved estimates of the thermal expansion component of sea-level rise are combined with estimates for

the other components (e.g. small glaciers), this bottom–up approach yields an estimate for sea-level rise of 1.5 mm yr^{-1} for the period 1961–2003, in good agreement with an independent estimate of 1.6 mm yr^{-1} (Domingues et al. 2008).

The observations that (i) the rate of sea-level rise has increased from 1.6 mm yr^{-1} in the period 1961–2003 to 3.1 mm yr^{-1} in the period 1993 2003 (Church and White 2006; Domingues et al. 2008) and (ii) sea-level rise is currently tracking at or near the upper limit of the IPCC projections (Figure 1c, Rahmstorf et al. 2007) have led to concern that mid range values of the IPCC projections could be significant underestimates. For example, a simple, semi-empirical approach to estimating future sea-level rise, which uses observations over the past 120 years to relate sea-level rise to global mean surface temperature, projects a range of sea-level rise for 2100 of 0.5 to 1.4 m above the 1990 level (Rahmstorf 2007; Figure 4). Although such statistical models do not include the process understanding that forms the basis for the model projections reported in the IPCC assessments, they may suggest that additional processes not yet incorporated in the more complex models are becoming important.

Much of the uncertainty about the rate of sea-level rise through the 21st century and beyond centres on the behaviour of the large polar ice sheets on Greenland and Antarctica. Although they have contributed only a small fraction of the observed sea-level rise to date (thermal expansion of the ocean and loss of ice from mountain glaciers and ice caps have been the most important factors (Domingues et al. 2008)), they have the potential to become much more important. Enough land-based ice is contained in the Greenland and West Antarctic ice sheets to raise global sea level by about 7 and 6 m, respectively, should both ice sheets completely disappear. The critical questions are (i) what level of temperature rise will lead to the loss of these ice sheets; and (ii) how fast can the ice be lost and thus sea level rise?

During the last interglacial (warm) period about 125,000 years ago, global mean sea level was about 4–6 m higher than it is today (e.g. Rostami et al. 2000; Muhs et al. 2002); loss of parts of both the Greenland and West Antarctic ice sheets were likely responsible (Overpeck et al. 2006). Global average temperature was about 1–2°C warmer during the last interglacial compared to the Holocene (the current interglacial), but regional temperatures near the

Figure 3. Projections of sea-level rise from 2100 from the IPCC Third Assessment Report and the Fourth Assessment Report (AR4).

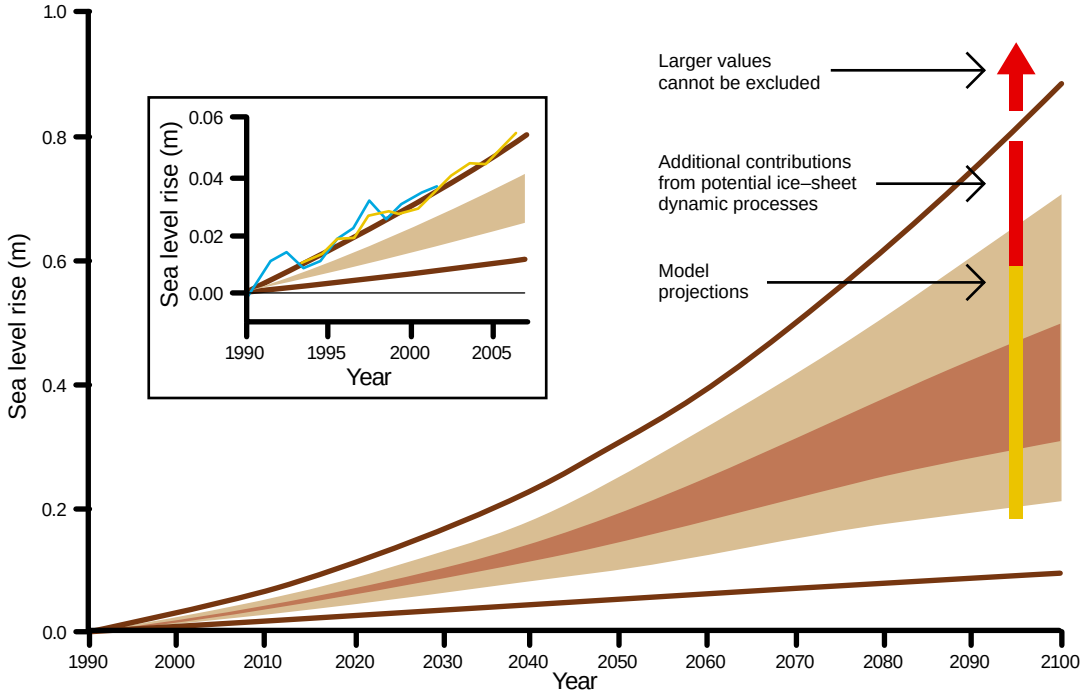

The Third Assessment Report projections are indicated by the shaded regions and the curved lines are the upper and lower limits. The AR4 projections are the bars plotted at 2095. The inset shows sea level observed with satellite altimeters from 1993 to 2006 (yellow) and observed with coastal sea-level measurements from 1990 to 2001 (blue). (Source: ACE CRC 2008)

Figure 4. Past sea level and sea-level projections.

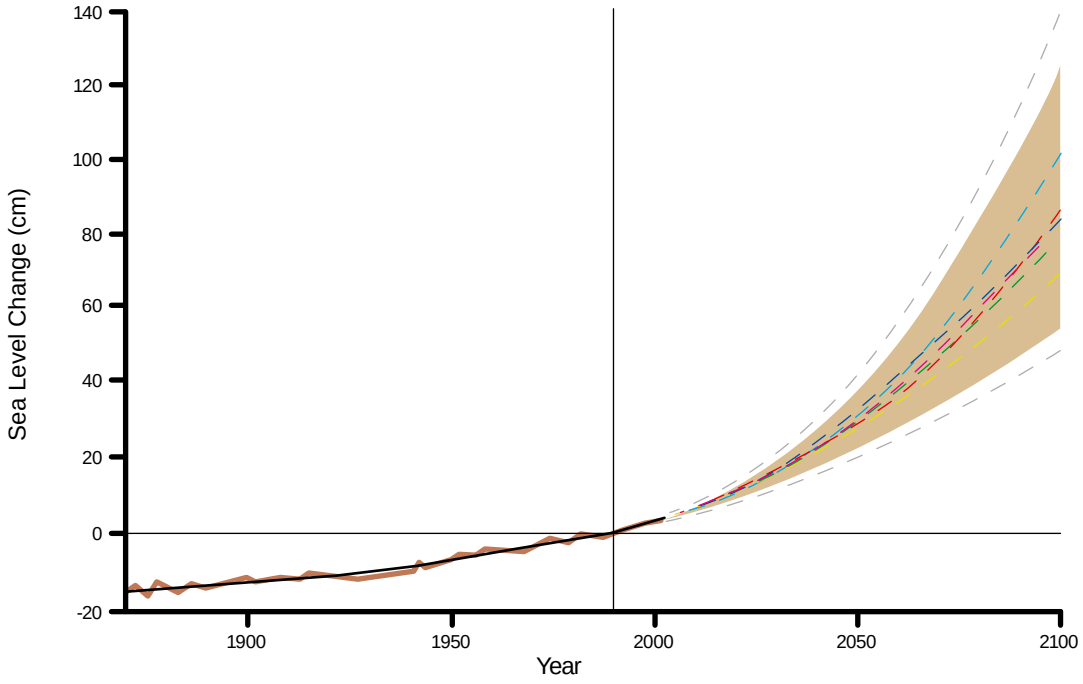

Projections from 1990 to 2100 based on global mean temperature projections of the IPCC Third Assessment Report. The brown uncertainty range spans the range of temperature rise of 1.4 to 5.8°C. The dashed grey lines show the added uncertainty due to statistical errors in the fit of the equation to data. Coloured lines are individual IPCC scenarios (e.g., light blue is the A1FI scenario, and the yellow line is the B1 scenario). (Source: Rahmstorf 2007, which includes more details on methodology)

poles were probably 3–5°C warmer. In addition, there was more direct solar insolation at the northern high latitudes than at present, which also contributed to the loss of part of the Greenland ice sheet (IPCC 2007).

At present global average temperature is about 0.8°C warmer than the pre-industrial value (IPCC 2007), but the temperature in the northern high latitudes has increased at almost twice that rate (ACIA 2004). If global average temperature rises to 1.9 to 4.6°C relative to pre-industrial, which is well within the range of the model projections (IPCC 2007), and is maintained for millennia within that range or higher, the Greenland ice sheet would largely be eliminated through surface melting *alone*; that is, the rate of surface melting would exceed the rate of snow accumulation during the winters (Gregory and Huybrechts 2006).

The *rate* of projected rise in sea level is critical for estimating the severity of potential impacts. Given sufficient foresight and ingenuity, society could arguably adapt to a sea-level rise of even 7 m, if spread over several millennia. However, post-AR4 research has suggested that dynamical processes can lead to more rapid loss of ice than by melting alone. Two processes are particularly important.

The first process is related to streams of melt water on the surface of the ice sheet. When these streams meet a crevasse, they can sometimes flow down to the base of the glacier, lubricating it and accelerating its movement towards the sea (Figure 5). This can produce large blocks of ice which, when they flow into the sea, cause an instantaneous rise in sea level through displacement of seawater. The process has been observed in recent years in Greenland (Das et al. 2008), with a number of estimates of the net mass balance of the ice sheet showing that over the past 15 years it has changed from being approximately in balance to now losing ice at a rate of 200 billion tonnes per year or greater (Figure 6; Rignot and Kanagaratnam 2006). However, the long-term importance of this process has been questioned by recent research (Holland et al. 2008; Nick et al. 2009).

The second process is related to the loss of ice shelves that form on the sea along the coastlines of polar land masses. This shelf ice acts to buttress the land-based outlet glaciers and slow their flow to the sea. When this shelf ice is lost, so too is the buttressing effect and the outlet glaciers often show a sharp increase in the rate of flow. The effect has been observed on the Antarctic Peninsula

Figure 5. Lubrication of a continental ice sheet.

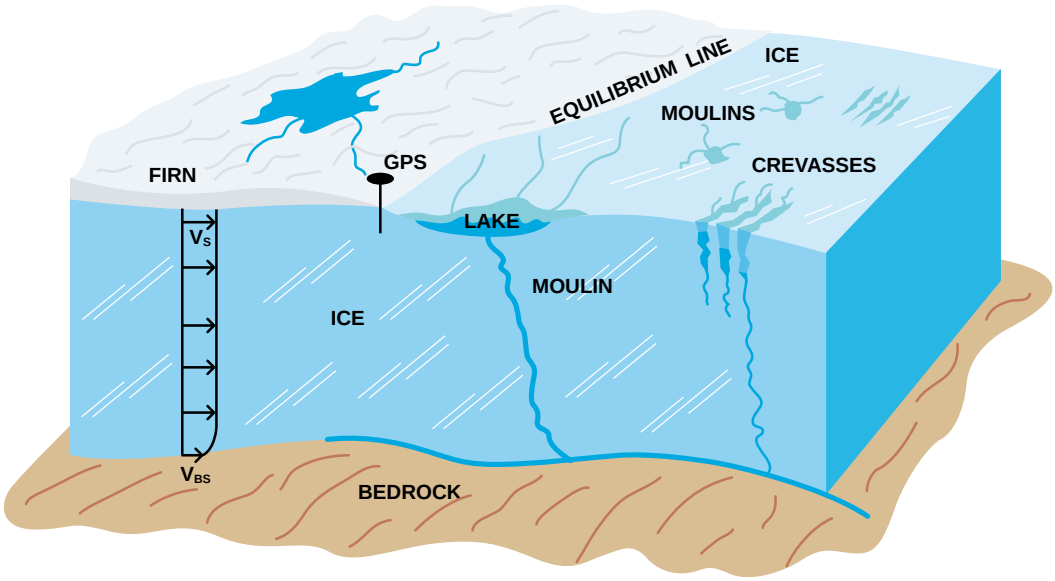

Lubrication is via transmission of melt water from the surface to the bedrock via crevasses and moulins. (Source: http://earthobservatory.nasa.gov/Newsroom/view.php?old=200206069411)

Figure 6. The areas of elevation gain and loss on Greenland.

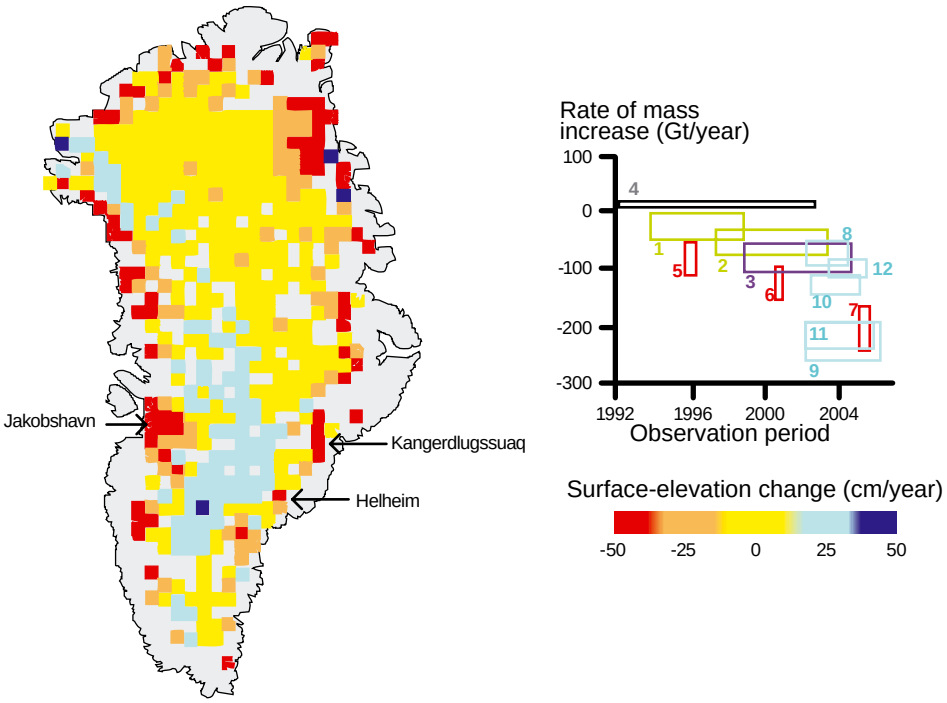

The graph shows rates at which the ice sheet is estimated to be changing based on airborne laser-altimeter surveys (green), airborne/satellite laser-altimeter surveys (purple), mass-budget calculations (red), and temporal changes in gravity (blue). Rectangles depict the time periods of observations (horizontal) and the upper and lower estimates of mass balance change (vertical). (Source: Konrad Steffen, National Snow and Ice Data Center, University of Colorado, USA)

(Figure 7; De Angelis and Skvarca (2003); Scambos et al. 2004). In the southern polar region the main concern is the West Antarctic ice sheet (with its ca. 6 m of equivalent sea level), which is grounded below sea level and where rising sea temperature can thus cause melting at the base of the ice sheet as well as undermining the stability of the buttressing ice shelves (Figure 8). A recent analysis shows warming of about 0.1°C per decade over the West Antarctica region over the last half century, attributed in part to changes in sea surface temperature (Steig et al. 2009). The West Antarctic ice sheet has shown relatively rapid periods of retreat and advance during climate oscillations in the past (Pollard and DeConto 2009), and appears to have collapsed during the Pliocene when planetary temperatures were about 3°C warmer than today (Naish et al. 2009).

Although these dynamical processes cannot yet be modelled quantitatively with any confidence, an analysis of the kinematic constraints on rapid ice discharge from land-based polar ice sheets has concluded that the maximum possible increase in sea-level rise by 2100 is around 2 m, but only under the most extreme levels of forcing (Pfeffer et al. 2008). A more plausible estimate of total sea-level rise by 2100 is around 0.8 m. This value lies at the upper end of the IPCC projections.

In summary, there is a considerable body of evidence now that points toward a sea-level rise of 0.5 to 1.0 m by 2100 compared to 1990 values. The main lines of argument include: (i) recent observations have confirmed the conclusion that sea level has been rising near the upper bound of the IPCC projections since 1990 (Rahmstorf et al. 2007; Domingues et al. 2008; Church et al. 2008); (ii) the mid range of the statistical projection of Rahmstorf (2007), based on observations, is 0.9 to 1.0 m; (iii) recent observations show increasing net mass loss from the Greenland ice sheet (Rignot and Kanagaratnam 2006) and the West Antarctic Ice Sheet (Cazenave 2006); (iv) physically based estimates of sea-level rise due to dynamical loss of ice from the polar ice sheets suggest that a 0.8 m rise is plausible (Pfeffer et al. 2008). Sea-level rise larger than the 0.5–1.0 m range – perhaps towards 1.5 m (i.e. at the upper range of the statistical projection of Rahmstorf 2007) – cannot be ruled out. There is still considerable uncertainty surrounding estimates of future sea-level rise. Nearly all of these uncertainties, however, operate in one direction, towards higher rather than lower estimates.

Figure 7: Glacier-ice shelf interactions.

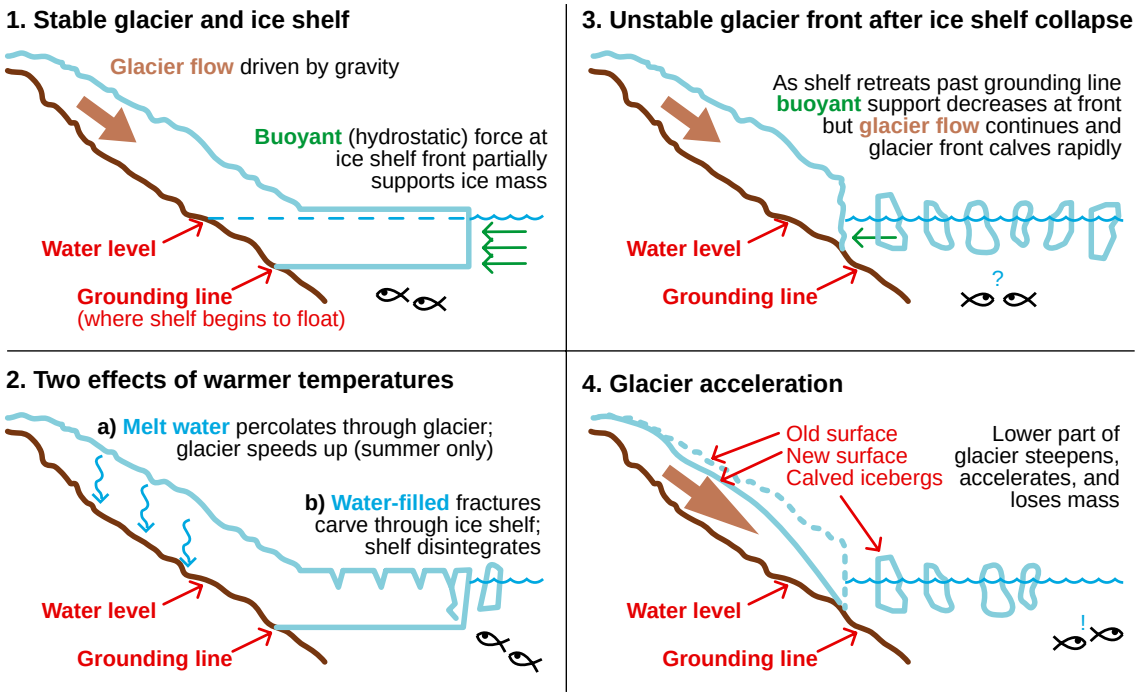

In a stable glacier-ice shelf system, the glacier's downhill movement is offset by the buoyant force of the water on the shelf. Warmer temperatures destabilise this system by lubricating the glacier's base and creating melt ponds that eventually carve through the shelf. Once the ice shelf retreats to the grounding line, the bouyant force that used to offset glacier flow becomes negligible, and the glacier speeds up on its way to the sea. (Source: Ted Scambos and Michon Scott, National Snow and Ice Data Center, University of Colorado, USA)

Figure 8. Profile through the Antarctic ice sheet.

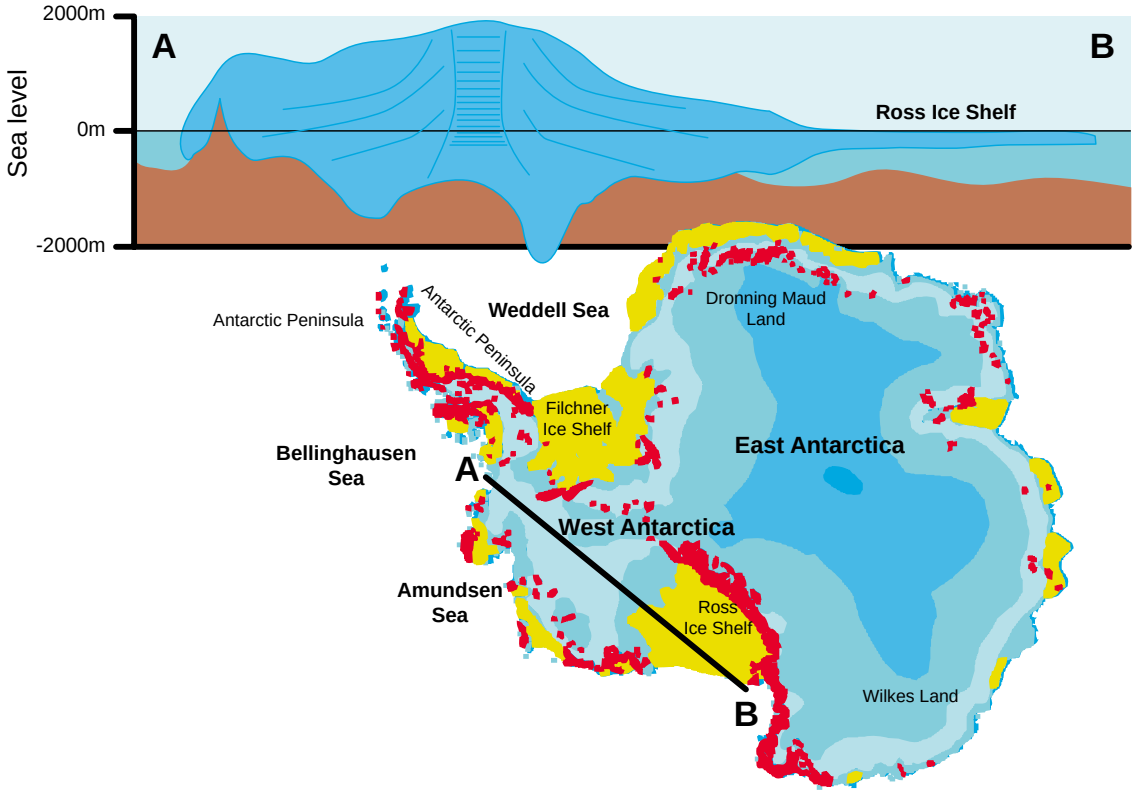

(A) Bellingshausen Sea – West Antarctic ice sheet – (B) Ross ice shelf – Ross Sea. The profile shows that most of the West Antarctic ice sheet is grounded below sea level which makes it sensitive to sea level rise. If the contact of the ice to the bottom rocks is lost seaward of the grounding line, the ice sheet becomes significantly thinner (some 100 m), forming shelf ice. The lines in profile are lines of similar age; annual layers in the center are thinning from top to bottom. Yellow areas: ice shelf. Red areas: not ice covered (2.8 % of total area). Blue shaded areas incremented by 1000 m in thickness. (Source: Hannes Grobe, Alfred Wegner Institute for Polar and Marine Research, Germany)

Although a 0.5 m rise in sea level over the century, which lies near the centre of the IPCC envelope of projections, may seem modest, the consequences can be surprisingly severe. Enhanced vulnerability to inundation of low-lying islands is a prominent example, but many coastlines around the world, especially sandy coastlines, will be subject to increased erosion and will retreat landwards. One of the more dramatic consequences of modest increases in sea level is the disproportionately large increase in the frequency of extreme sea-level events associated with high tides and storm surges. A 0.5 m rise in mean sea-level could cause such extreme events to occur hundreds of times more frequently by the end of the century (ACE CRC 2008; Figure 9); an event that now happens once every hundred years would be likely to occur two or three times per year.

Figure 9. The multiplying effect of sea level rise on high sea-level events.

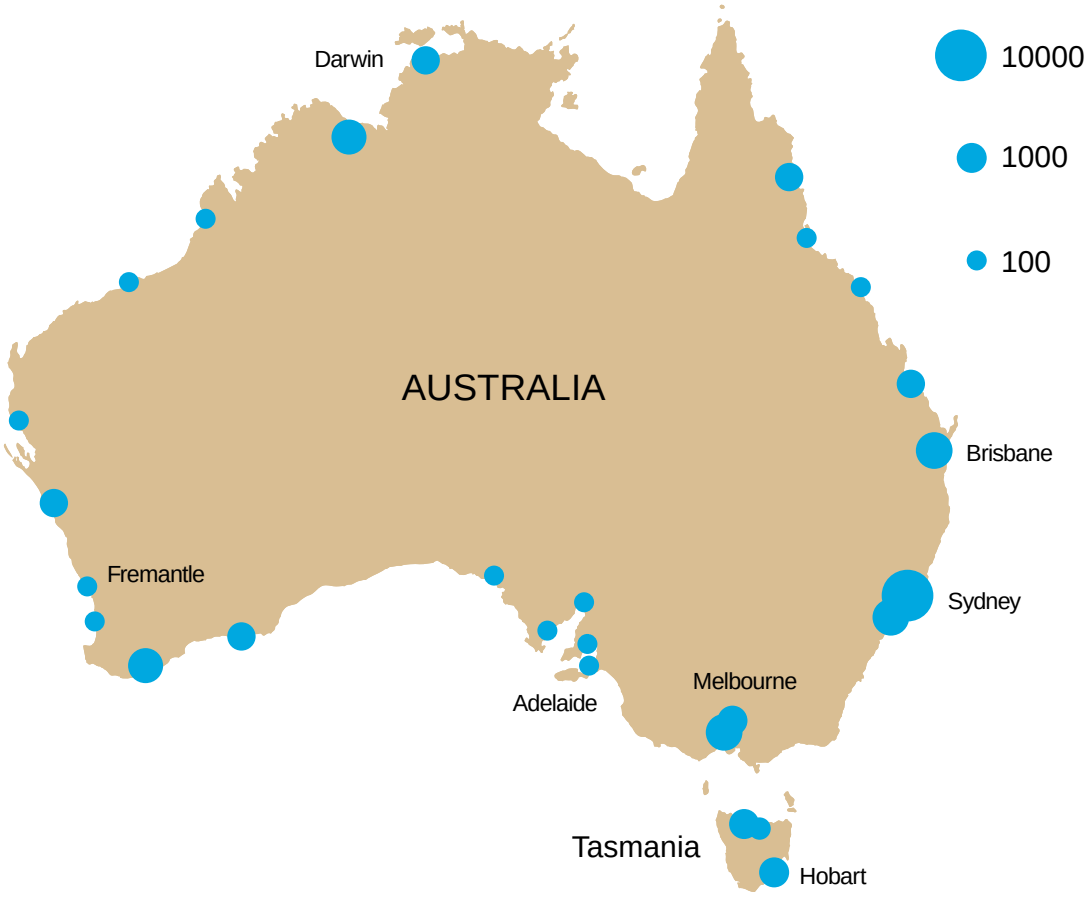

Estimated multiplying factor for the increase in the frequency of occurrence of high sea-level events with a sea-level rise of 0.5 m. (Source: ACE CRC 2008)

2.2 Changing water availability

The effect of climate change on the hydrological cycle, and the consequences for water resources, is one of the most important aspects of climate change for societies around the world, and particularly for Australia. Globally, a warming climate is leading to an enhancement of the hydrological cycle – more evaporation, an increasing amount of water vapour in the troposphere and more precipitation (IPCC 2007).

However, there are very large regional variations in the observed changes in the hydrological cycle. In particular, significant increases in rainfall have been observed in northern Europe, north and central Asia, and eastern North and South America. Drying is occurring around the Mediterranean, western North America, southern Africa, the Sahel and parts of southern Asia. Longer and more intense droughts have been observed over large areas in the tropics and sub-tropics since the 1970s (IPCC 2007). Although these trends cannot be linked to anthropogenic climate change with a high degree of

Figure 10: Trends in annual total rainfall (mm/10 years) across Australia.

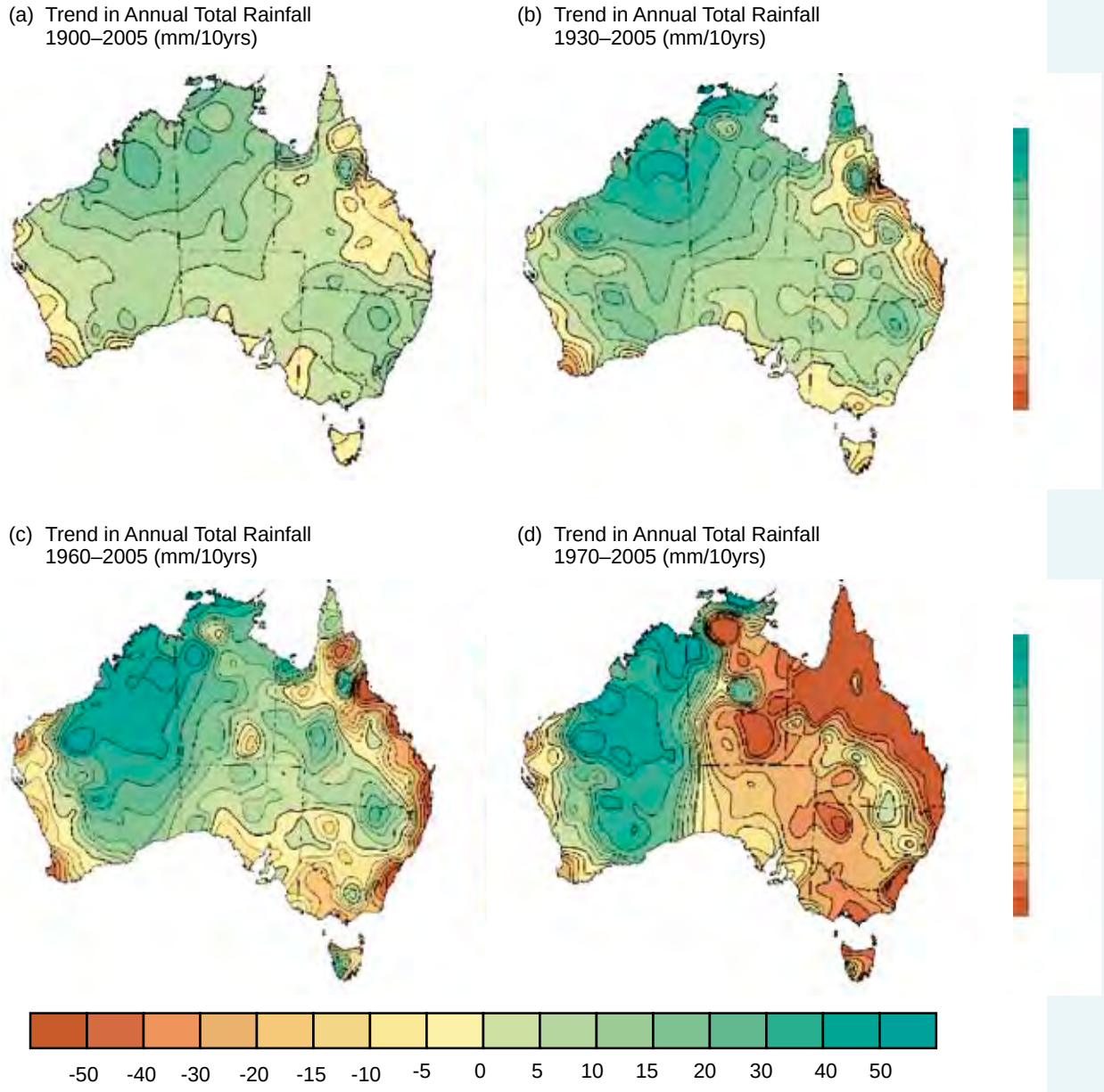

The maps relate to four time periods: (A) 1900–2005; (B) 1930–2005: (C) 1960–2005: (D) 1970–2005.
(Source: Australian Bureau of Meteorology)

certainty, one study now shows that human-induced changes in precipitation can be discerned at the scale of latitudinal bands (Zhang et al. 2007).

Over Australia as a whole, rainfall did not change much over the 20th century, but the continental average masks very significant regional and temporal trends (Smith 2004). While the north and west of the continent are experiencing increases in rainfall, other areas have experienced decreases. The abrupt drop of around 15% in rainfall in the south-west of Western Australia is now a well-known phenomenon (Bates et al. 2008). A more widespread change is the drying trend in the east and south of the continent (Figure 10). The trend began around the middle of the last century, but has accelerated since 1970. Embedded in this broad trend are more regionally specific changes; for example, rainfall across Victoria and southern South Australia has dropped significantly since the early 1990s.

These observed implications of changes in rainfall patterns and other hydrological changes have implications for water availability in rural areas and for urban water supplies. Attribution of these changes is explored in the following discussion, with a focus on the potential links to anthropogenic climate change. The discussion is centred primarily on three areas: the Murray-Darling Basin; the south-east corner of the continent, particularly Victoria and southern South Australia; and south-west Western Australia.

The consequences of the drying trend for the Murray-Darling Basin are becoming particularly acute. During the period 2000–07 the average annual inflow in the river system was 4,150 GL yr^{-1}, compared to a long-term post-1950 average of about 12,300 GL yr^{-1}. In the period April 2006 – March 2007, inflow hit a record low of only 770 GL yr^{-1} (Cai and Cowan 2008) (Figure 11). The effect of the reductions in inflow on the surface water storage (reservoirs, lakes, weirs, in-channel storage) of the Murray-Darling Basin is striking. Storage is now so low in the Murray-Darling Basin system that there is not enough water to meet critical human needs for 2009–10 (Freeman 2009).

Water resources are ultimately dependent on the integrated total water storage of a drainage basin (including soil and groundwater as well as surface water), one of the most notoriously difficult parameters to measure accurately. Recent advances in space-based measurements of very small changes in Earth's gravitational field allow observations to be made of changes in total water storage across large drainage basins. The approach has been used to estimate changes in quantities of surface and groundwater storage in the Murray-Darling Basin from 2002 to the present (LeBlanc et al. 2009). The

Figure 11. Monthly inflows into the Murray-Darling system.

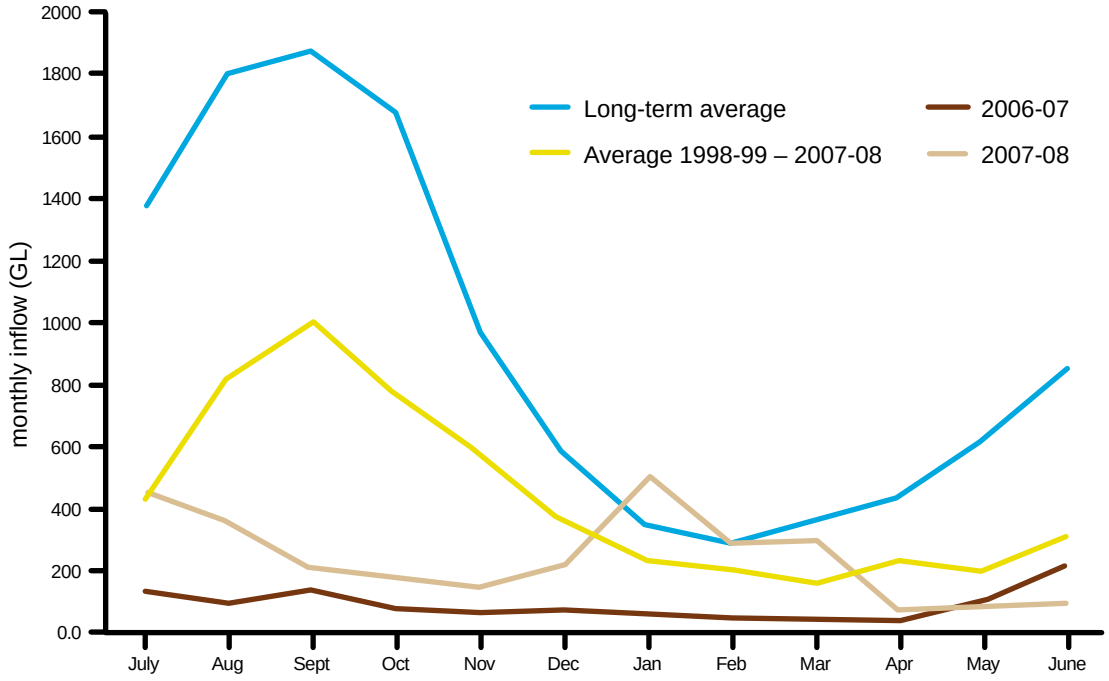

Observations for most recent years and decade compared to the long-term average. (Source: Murray-Darling Basin Commission)

work shows rapid drying of soil water and surface storages following the onset of drought in 2001, with persistent low levels reached in only two years (Figure 12). The water deficit worsened in 2005–06, and despite a return to average rainfall in 2007 and 2008, a substantial bulk water deficit remains across the Murray-Darling Basin.

The implications of the drying trend for urban water supplies are also profound. For example, over the past 10–15 years, the total volume of water in Melbourne's water storages has dropped sharply, from near full capacity in 1996 to well under half capacity in the period 2006–08 (Figure 13). Similar reductions in water supplies have been recorded for the other major cities in south-east Australia; for example, the May 2009 level as a percentage of full storage capacity for Adelaide is 54% and for Canberra 43.9%. Further north along the east coast there has been some recovery in urban water supplies (May 2009 levels of 58.4% for Sydney and 59.2% for Brisbane/south-east Queensland), due to increased rainfall in 2007–08. The reduction in the Perth water supplies occurred earlier, as an abrupt drop in the mid 1970s, with a possible further step-change in the 1990s (Figure 14).

A crucial question is the relationship of the observed drying trends in south-west Australia and the southern and eastern parts of the continent to anthropogenic climate change. Changes in both temperature and rainfall affect water availability. While changes in rainfall are more important for determining water availability, it is more straightforward to determine the link between rising temperature and reduced surface water availability. For example, since 1950 the streamflow in the Murray-Darling Basin has decreased by 55% while rainfall has decreased by only 11% (Figure 15). Although changes in rainfall are amplified in runoff, this alone cannot explain the large difference. An analysis of the 2001–07 drought, compared to earlier periods of low rainfall and inflow in the Murray-Darling Basin, suggests that a rise in temperature of 1°C could lead to a reduction in runoff of as much as 15%, even with no changes in rainfall (Cai and Cowan 2008). With increasing temperatures virtually certain for the coming decades and a significant probability of continued low rainfall according to General Circulation Model (GCM) projections, the Murray-Darling Basin will likely experience continuing low inflows to the middle of the century and beyond.

In terms of rainfall, the natural variability of Australia's climate is amongst the highest of any large region of the planet, and is strongly influenced by subtle changes in the surrounding oceans. Natural modes of climate variability, such as the El Niño – Southern Oscillation, the Indian Ocean Dipole and the Southern Annular Mode, play a strong role in the amount and pattern of rainfall across the continent. Severe droughts and drying trends have occurred in the past, before anthropogenic climate change could have been a major factor, making it difficult to determine the role of climate change in the current dry period.

Figure 12. Changes in total water volume of the Murray-Darling Basin.

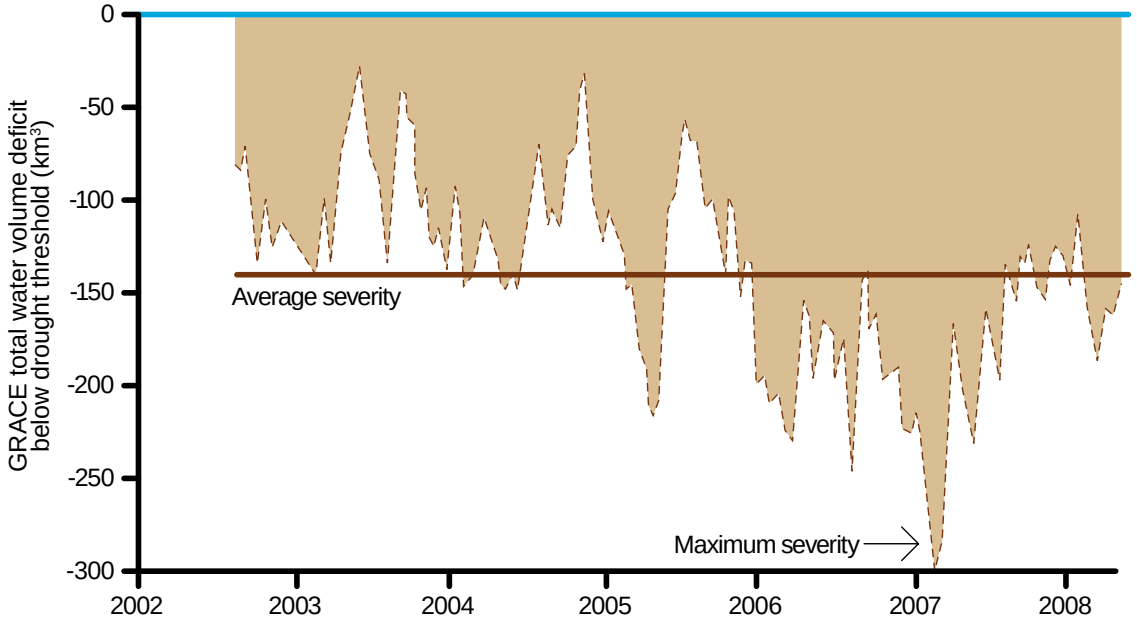

As estimated from GRACE (Gravity Recovery and Climate Experiment) measurements. (Source: LeBlanc et al. 2009)

Figure 13. Total volume of water in Melbourne's urban water storages from 1996 to 2008.

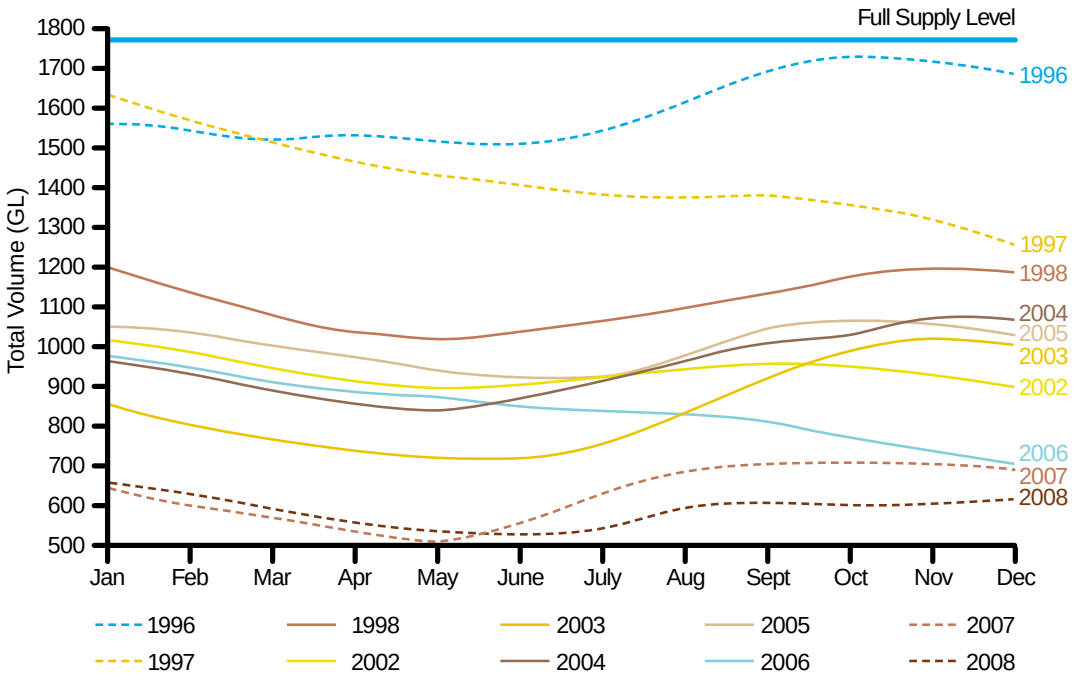

(Source: Melbourne Water)

Figure 14. Trends in total annual stream flow into Perth dams 1911–2008.

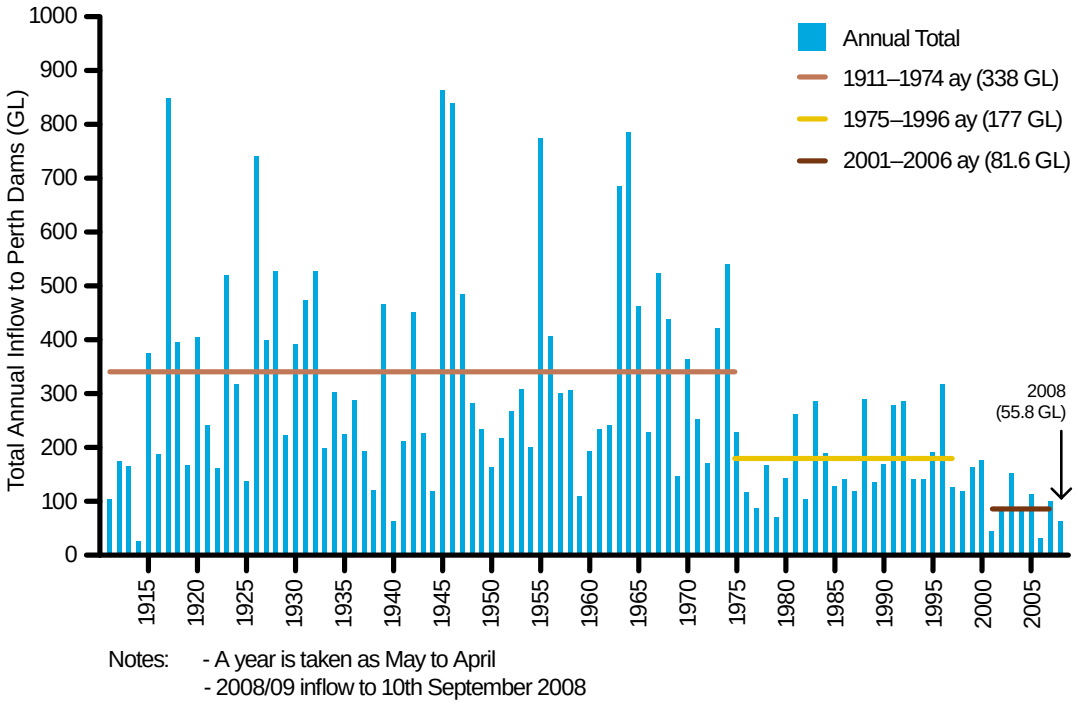

(Source: Western Australian Water Corporation)

Figure 15. Total annual inflow and rainfall in the Murray-Darling Basin (MDB).

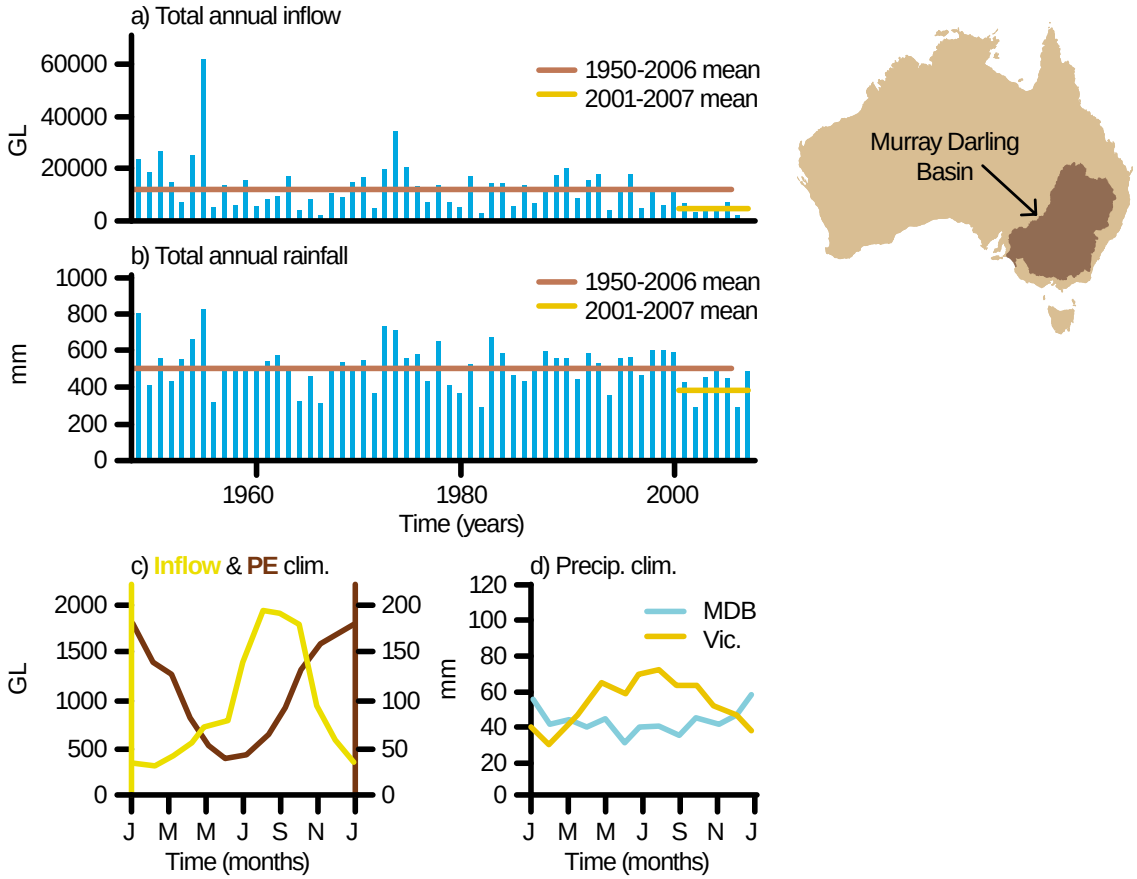

(a) Time series of annual total inflow to the MDB; (b) annual total rainfall averaged over the MDB. Annual cycle of (c) inflow (yellow line) and areal potential evaporation (brown line), and (d) rainfall over the MDB (blue line) and Victoria (orange line). (Source: Cai and Cowan 2008)

Considerable progress is being made, however, in the attribution challenge. For example, a concerted research effort over recent years has begun to untangle the factors that may be contributing to the drying of south-west Western Australia. There is strengthening evidence that changes in the Southern Annular Mode, a zonal pattern of variability often characterised by the pressure difference between 45° and 60°S, is a major contributor (Timbal et al. 2009; Nicholls 2009). In addition, Timbal et al. (2009) argue for a significant influence more recently of the sub tropical ridge, a zone of high pressure that often lies over the east of the continent and has strengthened considerably since 1970. There is plausible evidence that changes in both the Southern Annular Mode and the sub tropical ridge are linked to anthropogenic climate change (Timbal et al. 2009). Model projections for the future are also consistent with this observation (CSIRO and Bureau of Meteorology 2007).

Attribution of the drying trends in eastern and southern Australia are more difficult than for the south-west. Two aspects of the drying trend, however, are now reasonably well understood. First, the proximate cause of the drop in rainfall over the south-east Australian region is an increase in surface atmospheric pressure over the continent (Nicholls 2009). Second, any changes in the behaviour of the El Niño – Southern Oscillation over the last half century have little or nothing to do with the observed drying trend in the south-east (Ummenhofer et al. 2009; Nicholls 2008).

Changes in the other two major modes of natural variability – the Southern Annular Mode and the Indian Ocean Dipole – are probably closely linked to the observed drying trend in the south-east. An analysis of rainfall patterns in the region coupled with patterns of variability in sea surface temperatures in the Indian Ocean points towards an absence of sea surface temperature conditions that lead to enhanced tropical moisture transport across Australia as the primary reason for recent droughts (Ummenhofer et al. 2009; Figure 16). However, the increase in rainfall in north-west Australia argues against the

Figure 16. Historical record of the Indian Ocean Dipole (IOD) and El Niño Southern Oscillation (ENSO) years and mean climatic conditions over south-east Australia.

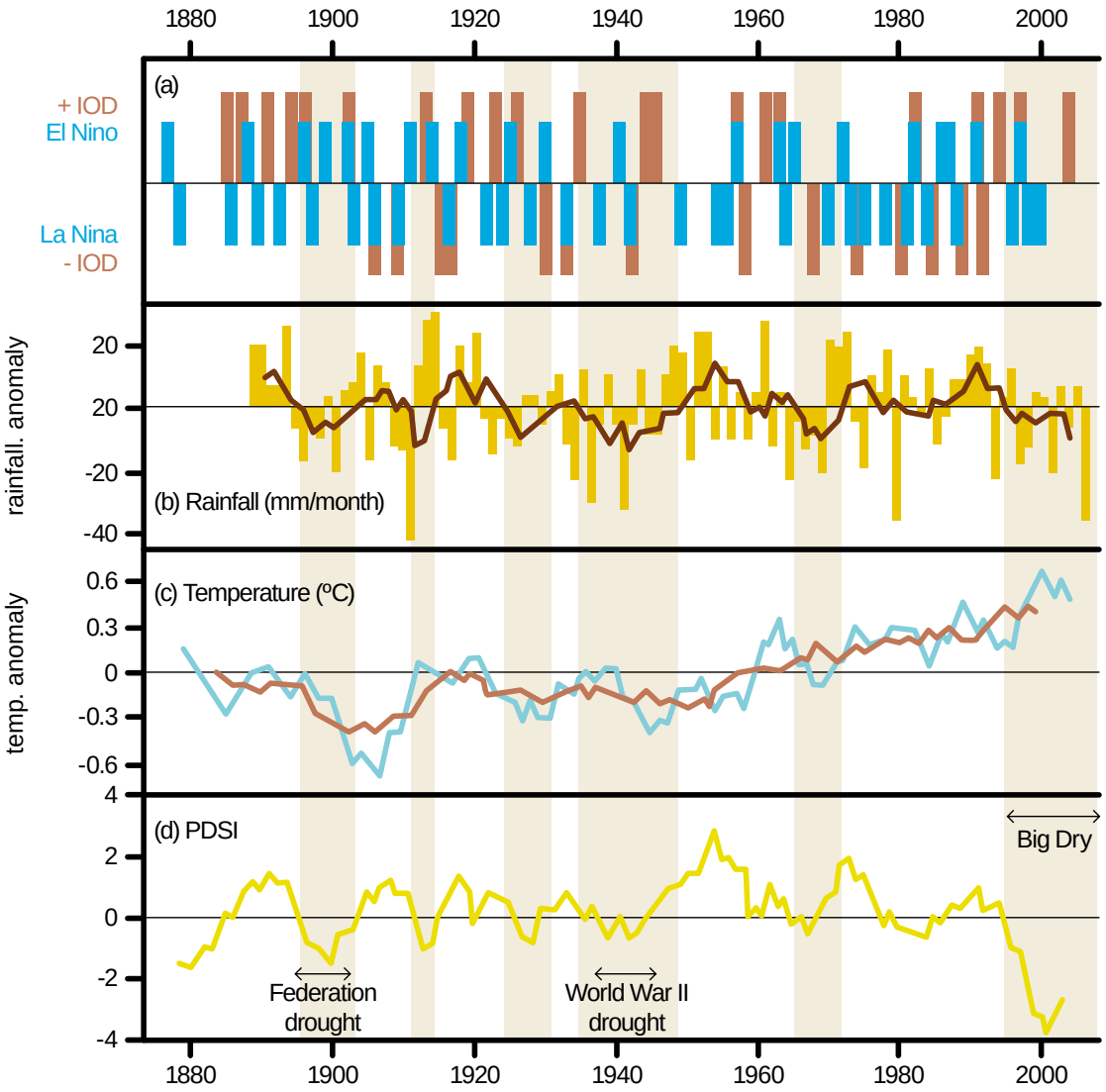

(a) Years of positive/negative IOD (brown) and El Niño/La Niña (blue) years. Timeseries of anomalous (b) precipitation (mm month-1), with 5-year running mean superimposed in red (c) 5-yr running mean of temperature (°C), with a 15-year running mean superimposed in brown, and (d) 5-yr running mean of Palmer Drought Severity Index (PDSI) over southeast Australia during June–October. The orange shaded bars highlight periods of below average precipitation when the 5-year running mean falls below one standard deviation. The duration of three major droughts has been indicated in (d) with horizontal black bars. (Source: Ummenhofer et al. 2009)

Indian Ocean Dipole – drought connection, as rainfall in both north-west and south-east Australia is normally influenced in the same direction by changes in the behaviour of the Indian Ocean Dipole (but see the discussion of the effect of Asian aerosols on Australian rainfall below).

An analysis of the link between changes in the Southern Annular Mode and dry conditions across all of southern Australia (south of 30°S) shows that trends in the Southern Annular Mode can account for 70% of the observed rainfall declines (Nicholls 2009). The strengthening of the subtropical ridge noted above also affects rainfall in the south-east, particularly in the Victoria – southern South Australia region (Timbal et al. 2009; Figure 17a,b). In fact, the causal link between warmer global temperatures, the increased intensity of the subtropical ridge, and the decreased rainfall in south-east Australia implies a high likelihood that the trend towards dry conditions will persist (SEACI 2007, 2008).

A recent attribution study (Baines 2009) that analysed the nature of decadal droughts in south-east Australia and three other regions of the world found that they are part of a global pattern of change in precipitation that is related to several modes of natural variability but also clearly carries an anthropogenic climate change signal. The analysis of long-term observations suggests that the changing precipitation pattern is related to the Atlantic Meridional Oscillation, the El Niño – Southern Oscillation and rising sea surface temperature, the latter linked to anthropogenic climate change.

The progress made in understanding the processes that contribute to the current drought and the longer-term drying trend in southern and eastern Australia provides insights into the reliability of model-based projections of future trends. For example, an analysis of model projections for the Australian region showed that the decrease in rainfall across southern Australia was accompanied by increased atmospheric pressures over the continent (Shi et al. 2008), consistent with the observations. Furthermore, the regional projections for Australia using a suite of models (CSIRO and Bureau of Meteorology 2007) show, with a very high level of consistency (up to 90%), a drop in winter rainfall for both south-west Western Australia and the Victoria/southern South Australia area. These projections mirror what has been occurring over these areas for the past several decades. For the Murray-Darling Basin, model projections show a 5 to 15% reduction in mean annual rainfall (mostly in winter and spring) by 2060 (Christensen et al. 2007), along with a warming trend in the eastern Indian Ocean Dipole; these projections are consistent with recent observations. Projections using only those GCMs that perform well in simulating current means and variability suggest a clustering of results at the drier end of the full set of model results, that is, a reduction of around 13% in rainfall (Smith and Chandler 2009).

The large amount of anthropogenic aerosols in the Asian region may also have an effect on rainfall in Australia, particularly the observed increase in rainfall in the north-west of the continent (Rotstayn et al. 2007, 2009). A GCM model experiment in which all forcings were included compared to runs where aerosol forcing was removed showed a substantial enhancement of rainfall over Australia when the effects of aerosols, particularly those over the Indian sub-continent, were included (Rostayn et al. 2007). The main effect is an indirect one, in which the Asian haze reduces the surface temperature over the sub-continent, altering the meridional temperature and pressure gradients over the Indian Ocean and thus leading to enhanced flow of monsoonal winds toward Australia.

Land-cover change – primarily the removal of forest cover – may also affect rainfall, particularly at local and regional scales. A continental-scale analysis of the effects of land-cover change on climate, based on climate model experiments, shows a statistically significant decrease in summer rainfall in south-east Australia, increased surface temperature during the 2002–03 El Niño event, and increased surface temperature in the eastern region of the continent (McAlpine et al. 2007). Modelling studies for south-west Western Australia, comparing the climate with natural and current land covers, suggest that the large-scale conversion of forests to agriculture in that region has contributed to a reduction in rainfall consistent with that observed and, as for the eastern Australia result, show surface warming associated with deforestation (Pitman et al. 2004; Timbal and Arblaster 2006). Land-cover change may also affect climatic extremes, with an increase in the number of hot, dry days, a decrease in daily rainfall intensity and an increase in drought duration (Deo et al. 2009).

In summary, rapid progress has been made in unravelling the interactions among modes of natural variability, factors such as land-cover change and Asian aerosols, and anthropogenic climate change in terms of Australia's hydrological cycle. The evidence is now strong for a climate change signal in the drying of south-west Western Australia. There is also some evidence for a climate change signal in the observed drying trend in Victoria and southern South Australia, although it is not as strong as in Western Australia. A climate change – drying connection further north along the east coast is not yet clear. The consequences of these trends, and their causes, for water supplies in urban Australia, for agriculture in the south-east and for the environment are serious, with the economic and social costs of adapting to ongoing warming and drying likely to rise sharply. As the evidence for a causal link between climate change and drying increases, so do the risks for the future of the most populous and agriculturally productive parts of Australia.

Figure 17. The link between drought in the southwest part of eastern Australia and the subtropical ridge.

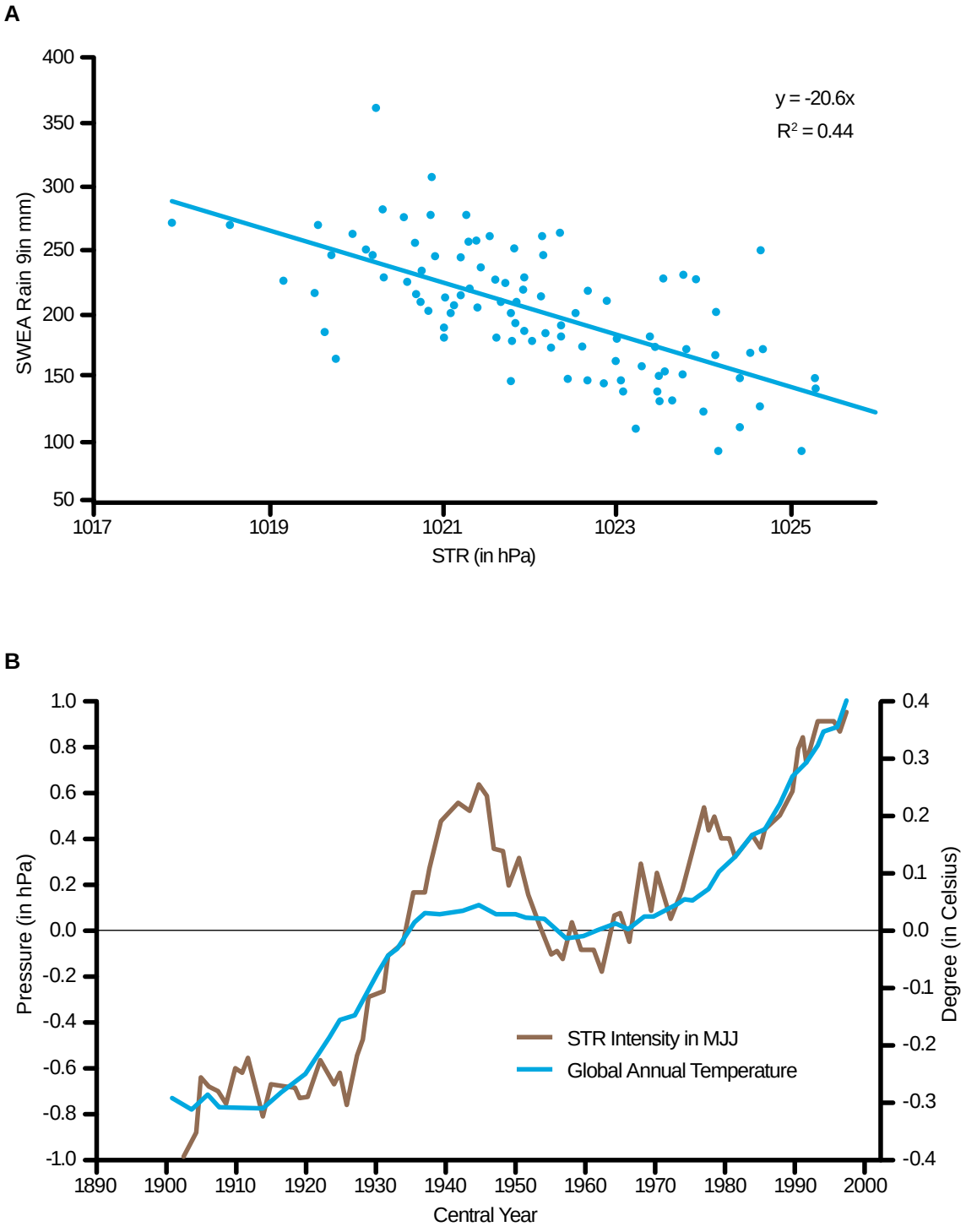

(A) Relationship between the May–June–July (MJJ) rainfall in the south west part of eastern Australia and the sub tropical ridge intensity during the same three months. The slope of the linear relationship and the amount of explained variance (r^2) is shown in the upper right corner. (B) Long-term (21-year running mean) evolution of the Sub-Tropical Ridge MJJ mean intensity (anomalies in hPa shown on the left-hand Y-axis) compared with the global annual surface temperature. (Source: Timbal et al. 2009, including further details on methodology)

2.3 Ocean acidification

About 25% of human emissions of CO_2 is absorbed by the oceans, a process that acts as a brake on the rate at which the climate is changing. However, as CO_2 dissolves into seawater, it increases the acidity (lowers the pH) of the ocean by formation of carbonic acid (Figure 18). Because the concentration of carbonate ions is related to the acidity of seawater, marine organisms that use dissolved carbonate ions to build solid calcium carbonate shells, such as corals, oysters, sea urchins, mussels, crustaceans and some forms of plankton, are sensitive to the pH of the ocean. Higher acidity (lower pH) reduces the saturation state of aragonite (a form of calcium carbonate) and makes it more difficult for these organisms to form shells.

The pH of the ocean has already changed significantly since the pre-industrial era (Guinotte et al. 2003), and is now about 0.1 pH unit lower (the pH scale is logarithmic so a change of 1 pH unit corresponds to a 10-fold change in acidity). This change in acidity corresponds to a drop in carbonate ion concentration of about 30 µmol kg^{-1} of seawater, to a present-day concentration of about 210 µmol kg^{-1}. This concentration is approaching the levels at which the aragonite saturation state becomes unfavourable for corals, the rate of calcification of marine organisms in general drops, and erosion of existing calcium carbonate shells begins (Hoegh-Guldberg et al. 2007).

The effects of the increased acidity in the ocean can already be observed in some biological systems (Moy et al. 2009). Furthermore, an observational study of seasonal variation in pH and carbonate ion concentration in the Southern Ocean shows an intense minimum in carbonate ion concentration in winter, suggesting that conditions deleterious for the growth of important calcifying plankton species could occur as early as 2030 in winter (McNeil and Matear 2008; Figure 19), and more generally by 2050–60

Figure 18. Linkages between the buildup of atmopsheric CO_2, the increase in ocean acidity and the decrease in carbonate ion concentration.

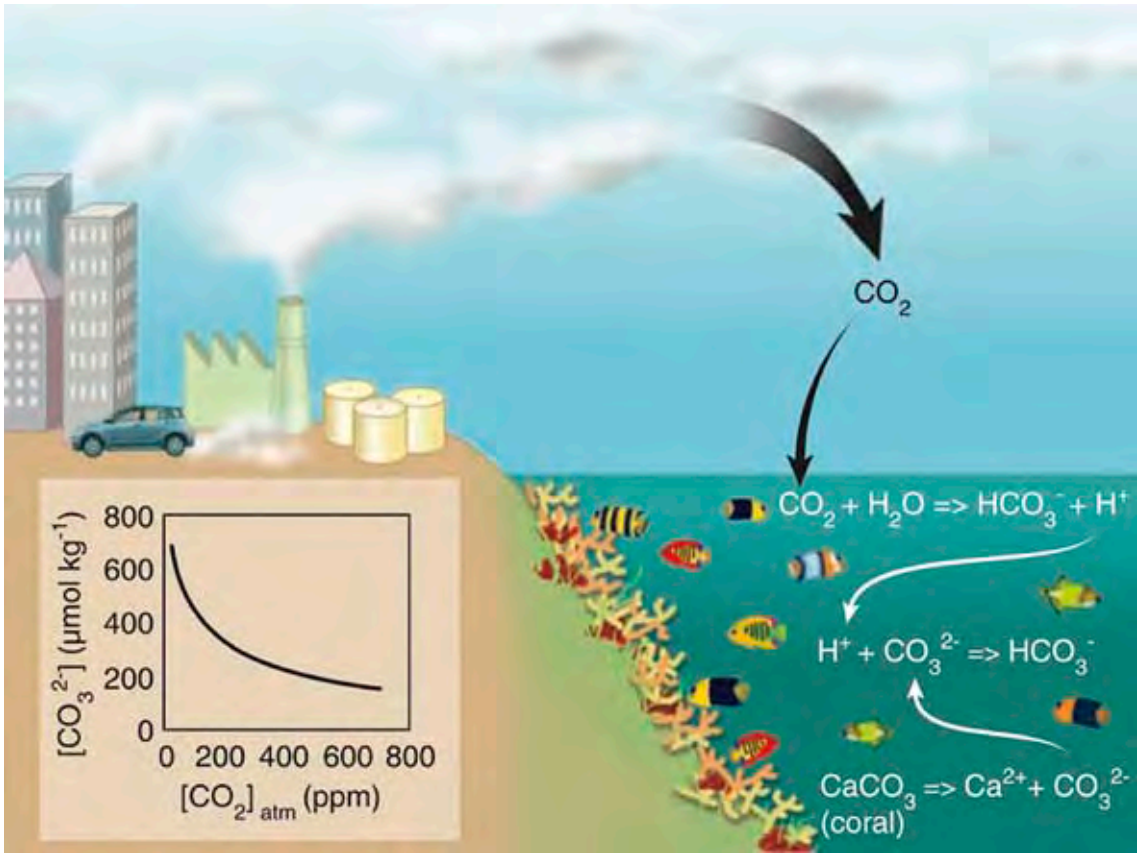

Approximately 25% of the CO_2 emitted by humans in the period 2000 to 2006 was taken up by the ocean where it combined with water to produce carbonic acid, which releases a proton that combines with a carbonate ion. This decreases the concentration of carbonate, making it unavailable to marine organisms that form calcium carbonate shells. (Source: Hoegh-Guldberg et al. 2007)

Figure 19. Undersaturation of aragonite.

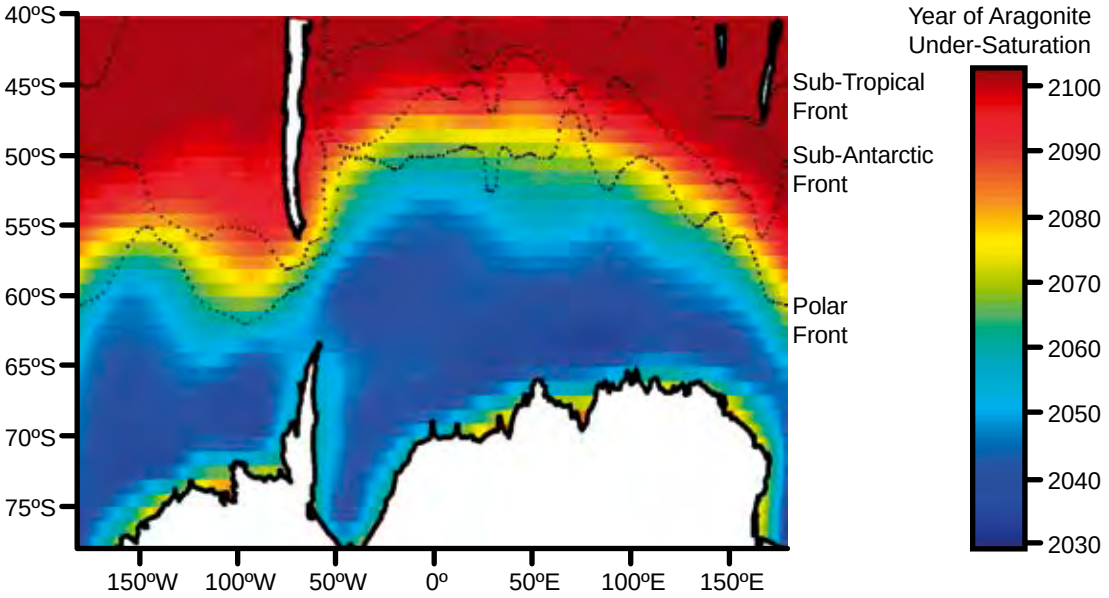

Contour plot of the year in which the onset of wintertime undersaturation of aragonite occurs under equilibrium conditions. Shown are average locations of Southern Ocean fronts. (Source: McNeil and Matear 2008)

(Orr et al. 2005). A widespread set of observations in the Great Barrier Reef involving 328 sites on 69 reefs shows that the rate of calcification of the coral *Porites* has declined by 14% since 1990, a very rapid and severe decline (De'ath et al. 2009; Figure 20). The decline is likely due to a combination of declining carbonate ion concentration and increased sea surface temperature.

Much of the concern about ocean acidification has focussed on coral reefs, such as the Great Barrier Reef. The combination of acidification, driven directly by rising atmospheric CO_2 concentrations, and rising sea surface temperatures, driven indirectly in part by rising CO_2 concentrations, presents a double whammy (Anthony et al. 2008). The best approach to maintaining healthy reefs in the face of these physico-chemical stressors is to increase

Figure 20. The impact of ocean acidity on Porites.

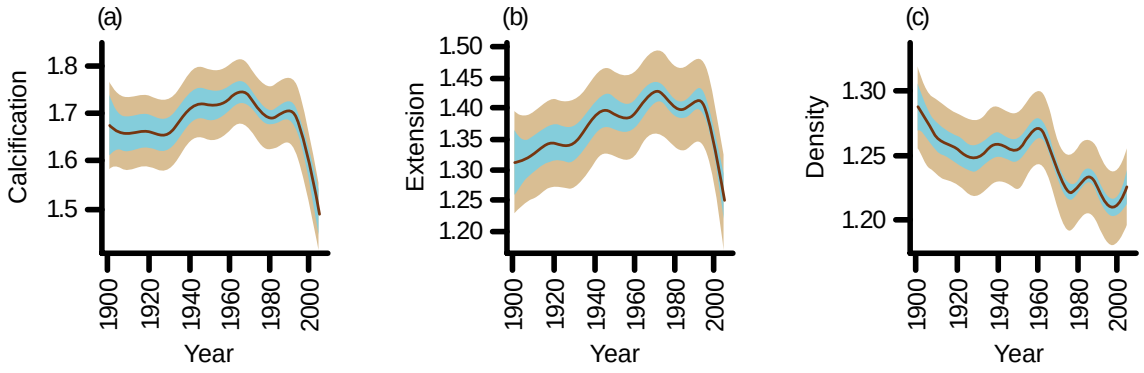

Variation of (A) calcification (grams per square centimetre per year), (B) linear extension (centimetres per year) and (C) density (grams per cubic centimetre) in Porites over time. Blue bands indicate 95% confidence intervals for comparison between years, and brown bands indicate 95% confidence intervals for the predicted value for any given year. (Source: De'ath et al. 2009)

the resilience of the reefs by controlling or removing other stressors (e.g. fishing pressure, nutrient inflows from adjacent land) as far as possible and by maintaining high levels of biodiversity (Hughes et al. 2003). This approach has so far minimised impacts on the Great Barrier Reef. However, there are limits to this approach, and business-as-usual trajectories of increasing acidity and sea surface temperature will likely overwhelm even the most resilient of reefs sometime in the second half of the century (Hoegh-Guldberg et al. 2007; Figure 21).

Figure 21. Temperature, atmospheric CO_2 concentration and carbonate ion concentrations reconstructed for the past 420,000 years.

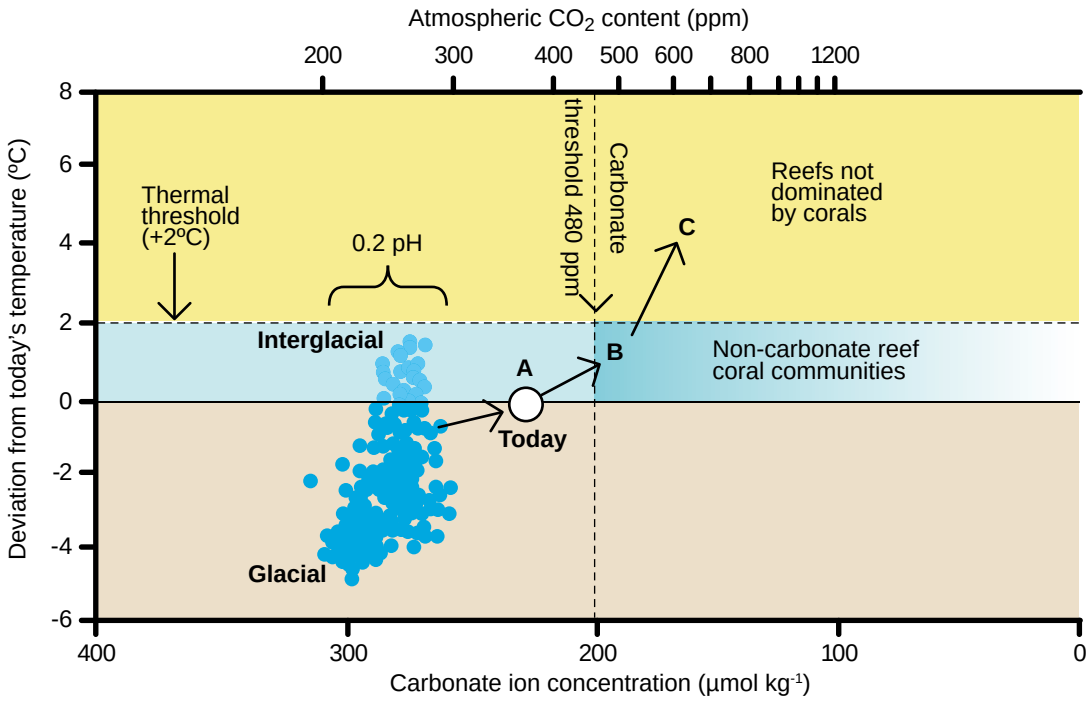

Carbonate concentrations were calculated from Vostok ice core data. Acidity of the ocean has varied by +/- 0.1 pH units over the past 420,000 years. The thresholds for major changes to coral communities are indicated for thermal stress (+2°C) and carbonate ion concentration of 200 micro-mol kg^{-1} , which corresponds to an approximate aragonite saturation Ωarag of 3.3 and an atmospheric CO_2 concentration of 480 parts per million (ppm). Black arrows pointing towards the upper right indicate the pathway currently followed towards atmospheric CO_2 concentration of more than 500 ppm. The letters A, B and C refer to reef states described in the figure. (Source: Hoegh-Guldberg et al. 2007, including details of the reconstructions)

2.4 Storms and extreme events

Extreme events, such as storms, floods, fires and droughts, are manifestations of the climate system with immediate and obvious impacts on people, infrastructure and ecosystems. Model-based projections of future climate show an increase in the frequency and severity of most types of extreme events, and suggest that shifts in the patterns of some extreme events should be observable by now. However, it is difficult to determine whether, in fact, extreme events have been increasing over the past several decades, primarily due to the quality and length of the data sets needed to detect significant changes in infrequent events.

Efforts to collect reliable data have improved in some countries since the mid 1990s, allowing the IPCC AR4 2007 to begin to discern some trends. It is very likely that hot days/nights have become more frequent and cold days/nights less frequent over land areas during the last half-century (Figure 22), with heatwaves also likely to have increased. Both heavy precipitation events and the areas of land affected by drought have likely increased since 1950. The incidence of high sea-level events has also probably increased worldwide since 1975 (Woodworth and Blackman 2004; Church et al. 2006).

Data on temperature-related extremes are the most readily available. Several extreme heatwaves have been documented over the past decade. The central European heatwave of 2003 which led to about 30,000 excess deaths is the most well known. Australia has also experienced severe heatwaves; the February 2004 event in south-east Australia was meteorologically as severe as the European event but caused many fewer deaths due to the lower vulnerability of the Australian population. Melbourne experienced a record high temperature of 46.6°C in February 2009, and recorded an unprecedented three consecutive days of 43°C or above in late January 2009. During this period Canberra experienced a record three consecutive days of 40°C temperatures. Adelaide also recorded record extreme temperature events in the 2008–09 summer, with a high temperature for February 2009 of 44.2°C and eight days above 35°C during the month (the average for February is four to five days above 35°C). A new record for high minimum temperature – 33.9°C – was set in the Adelaide region.

Figure 22. Australian average number of hot days/nights and cold days/nights.

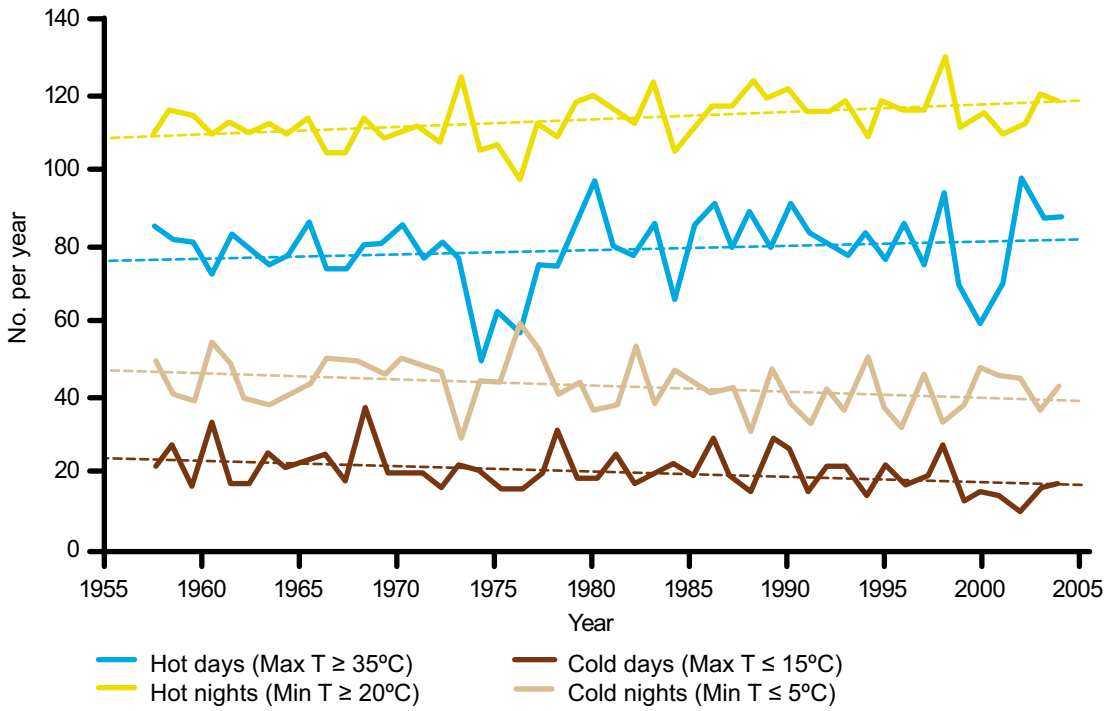

Hot days (daily maximum temperature ≥ 35°C), cold days (daily maximum temperature ≤ 15°C), hot nights (daily minimum temperature ≥ 20°C) and cold nights (daily minimum temperature ≤ 5°C) per year. Annual averages of extreme events are based on only observation sites that have recorded at least one extreme event per year for more than 80% of their years of record. Dashed lines represent linear lines of best fit. (Source: Data from N. Nicholls, published in Steffen et al. 2006)

Heatwaves such as the 2009 south-east Australian event can have important implications for infrastructure. The Basslink interconnecter, a submarine power cable that connects Tasmania to the mainland, experienced a “protective shutdown” during the 2009 heatwave when its design limits for temperature extremes were exceeded (Basslink 2009). The upper temperature limits for normal cable operation are 43°C in Victoria and 33°C in Tasmania. The upper limits were exceeded on both ends of the cable, with George Town in Tasmania recording a record high of 35°C in January 2009.

Globally, heat extremes will have increasingly serious implications for food security as they affect the production of food. An analysis of observed reductions in food production in the past due to unusually high temperatures during the growing season (e.g. 21–36% during the 2003 European heatwave) give an indication of the drops in production that, without effective adaptation and the development of new, heat-tolerant crops, could be expected later this century (Battisti and Naylor 2009). Tropical and subtropical regions, where food insecurity is already high, will be particularly affected. There is a greater than 90% probability that normal growing season temperatures globally near the end of the 21st century will exceed the most extreme seasonal temperatures recorded in the period 1900–2006 (Battisti and Naylor 2009; Figures 23 and 24).

The observational evidence for an increase in heavy precipitation is not so strong as that for high temperatures, but recent work has strengthened the case for a change towards more intense events. A comparison of satellite observations with model simulations of tropical precipitation events has shown a clear link between temperature and rainfall extremes (Allan and Soden 2008; Figure 25). Heavy rainfall events increase during warm periods. Interestingly, the observed amplification of rainfall events during warm periods is larger than that simulated by climate models. Consistent with the Allan and Soden work is an observational study based on infra-red satellite technology that has detected an increase in thunderheads over tropical oceans, with a 45% increase in thunderhead formation correlated with a 1°C increase in sea surface temperature (Aumann et al. 2008). However, in areas showing decreases in average rainfall, the trend towards heavy precipitation events is not often observed (e.g. Alexander et al. 2007).

Earlier reports of a link between the intensity of hurricanes (tropical cyclones) in the Atlantic Ocean with sea surface temperature (Emanuel 2005; Elsner et al. 2008; Saunders and Lea 2008) has triggered a flurry of research into the relationship between tropical cyclones and climate change. While the relationship between intensity of tropical cyclones and sea surface temperatures is now more widely accepted, at least for the Atlantic, the continuation of

Figure 23. Northern Hemisphere summer average observed and projected temperatures for France, Ukraine and the Sahel.

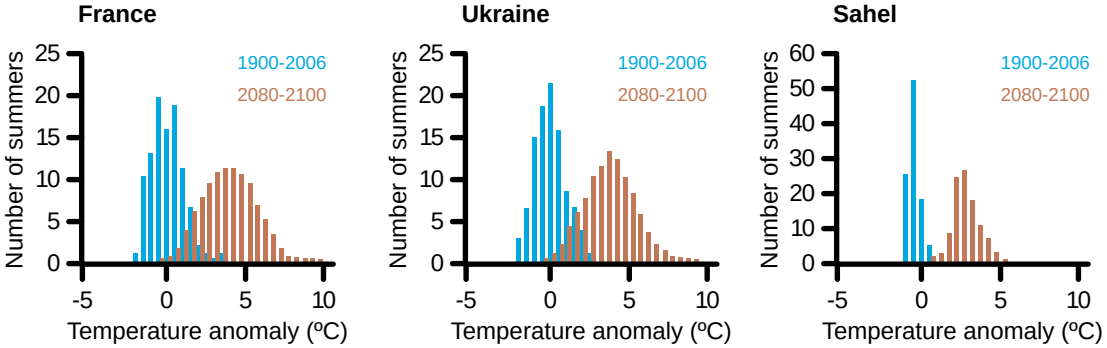

Histogram of northern hemisphere summer (June, July, August) averaged temperatures (blue) observed from 1900 to 2006 and (brown) projected for 2090 for (A) France, (B) Ukraine, and (C) the Sahel. Temperature is plotted as the departure from the long-term (1900–2006) climatological mean. The data are normalised to represent 100 seasons in each histogram. In (A), for example, the hottest summer on record in France (2003) is 3.6 °C above the long-term climatology. The average summer temperature in 2090 is projected to be 3.7 °C greater than the long-term climatological average, and there is a small chance it could be 9.8 °C higher. (Source: Battisti and Naylor 2009)

Figure 24. Likelihood that summer temperatures will exceed the current observed record.

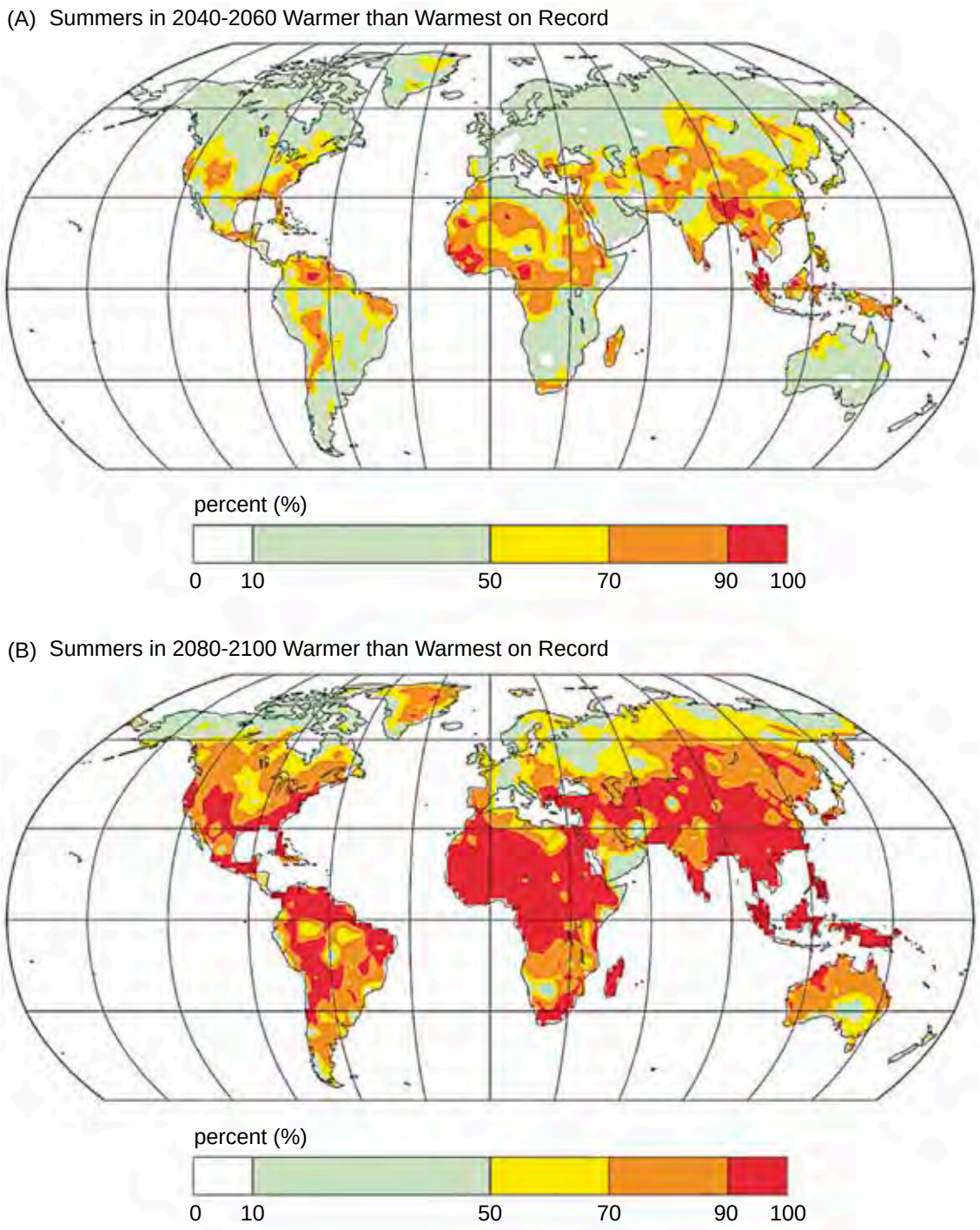

Likelihood (in percent) that future summer average temperatures will exceed the highest summer temperature observed on record in (A) 2040–2060 and (B) 2080–2100. For example, for places shown in red there is greater than a 90% chance that the summer-averaged temperature will exceed the highest temperature on record (1900–2006). (Source: Battisti and Naylor 2009)

the causal link into the future has been questioned. The critical issue is whether the observed increase in hurricane intensity in the Atlantic is due to the relatively higher increase in sea surface temperatures in the Atlantic relative to other ocean basins or whether it is related directly to the absolute increase in sea surface temperatures, regardless of what is happening in other ocean basins (Vecchi et al. 2008; Figure 26). If tropical cyclone intensity is linked to relative sea surface temperatures, then the intensity might relax to earlier levels as inter-ocean basin sea surface temperatures equilibrate. On the other hand, if intensity is related to absolute sea surface temperatures, then the link between climate change and cyclone intensity is strong, with even more intense cyclones expected later this century. The observational record is not yet long enough, and the basic process-level understanding is not yet good enough, to distinguish between these two possible futures.

Bushfires are one of the most deadly types of climate-related extreme events for Australia. In the past decade south-east Australia has experienced two megafires. The 2003 event destroyed 500 homes in suburban Canberra and left three people dead. The February 2009 fires in Victoria were an unprecedented catastrophe, killing 173 people and leaving the entire nation in deep shock.

The link between climate change and bushfires is multi-faceted and complex, and thus more difficult to establish than the connection between climate change and heatwaves, heavy precipitation events or tropical cyclones. Bushfires and their impacts are influenced by many factors, including the amount and condition of the fuel load (vegetation), the vulnerability of people and infrastructure, land-cover patterns, invasions of exotic species, extreme weather events, ignition sources, and management practices (such as prescribed burning to reduce fuel loads).

Climate change affects most of these factors and thus influences fire regimes in many ways (Williams et al. 2009; Lucas et al. 2007). Changing precipitation patterns, higher temperatures and increasing atmospheric CO_2 concentrations all influence vegetation growth, driving both changes in productivity and biomass and shifts in ecosystem composition. The warming and drying trend in south-east Australia has made the fuel load, whatever its biomass and composition, more susceptible to burning. Extreme fire weather days, those with extreme temperatures and high winds, are becoming more likely under a warming climate. The overall effect, which is generally towards a higher risk of large and intense fires, is difficult to estimate precisely, and can perhaps best be assessed using analysis of historical observations along with models that simulate fire behaviour under various climatic regimes.

Figure 25. The link between sea surface temperature (SST) and rainfall extremes.

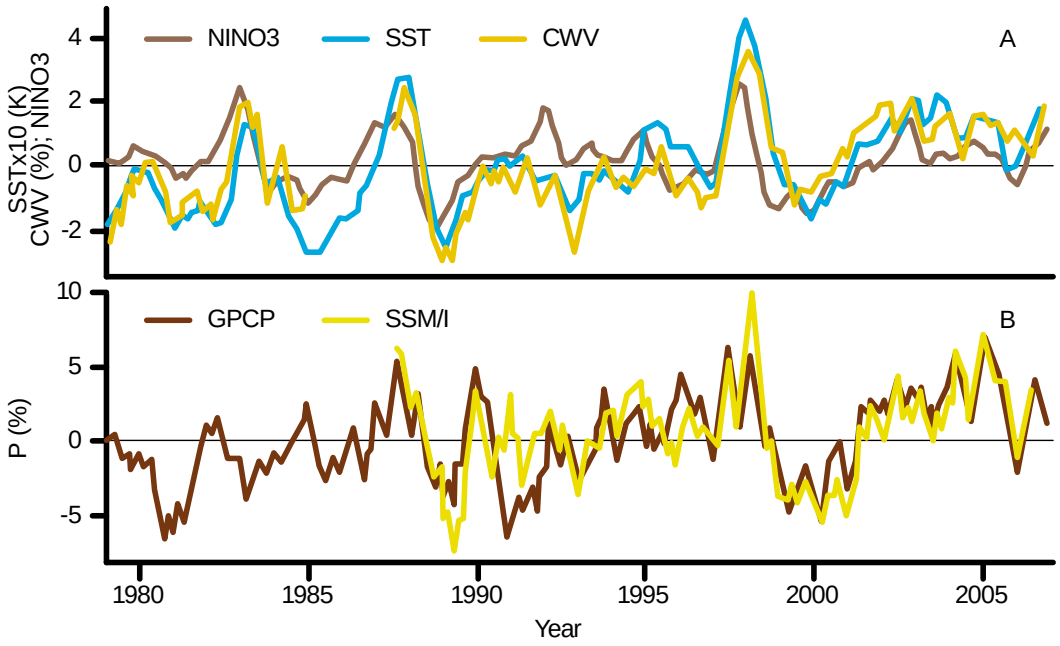

Time series of (A) Nino-3 ENSO index (SST anomalies for 90° to 150°W, 5°S to 5°N region), deseasonalised tropical ocean (30°S to 30°N) mean anomalies of SST, and column-integrated water vapour (CWV); and (B) preciptation (P). (Source: Allan and Soden 2008)

Figure 26. Past and extrapolated changes in Atlantic hurricane activity.

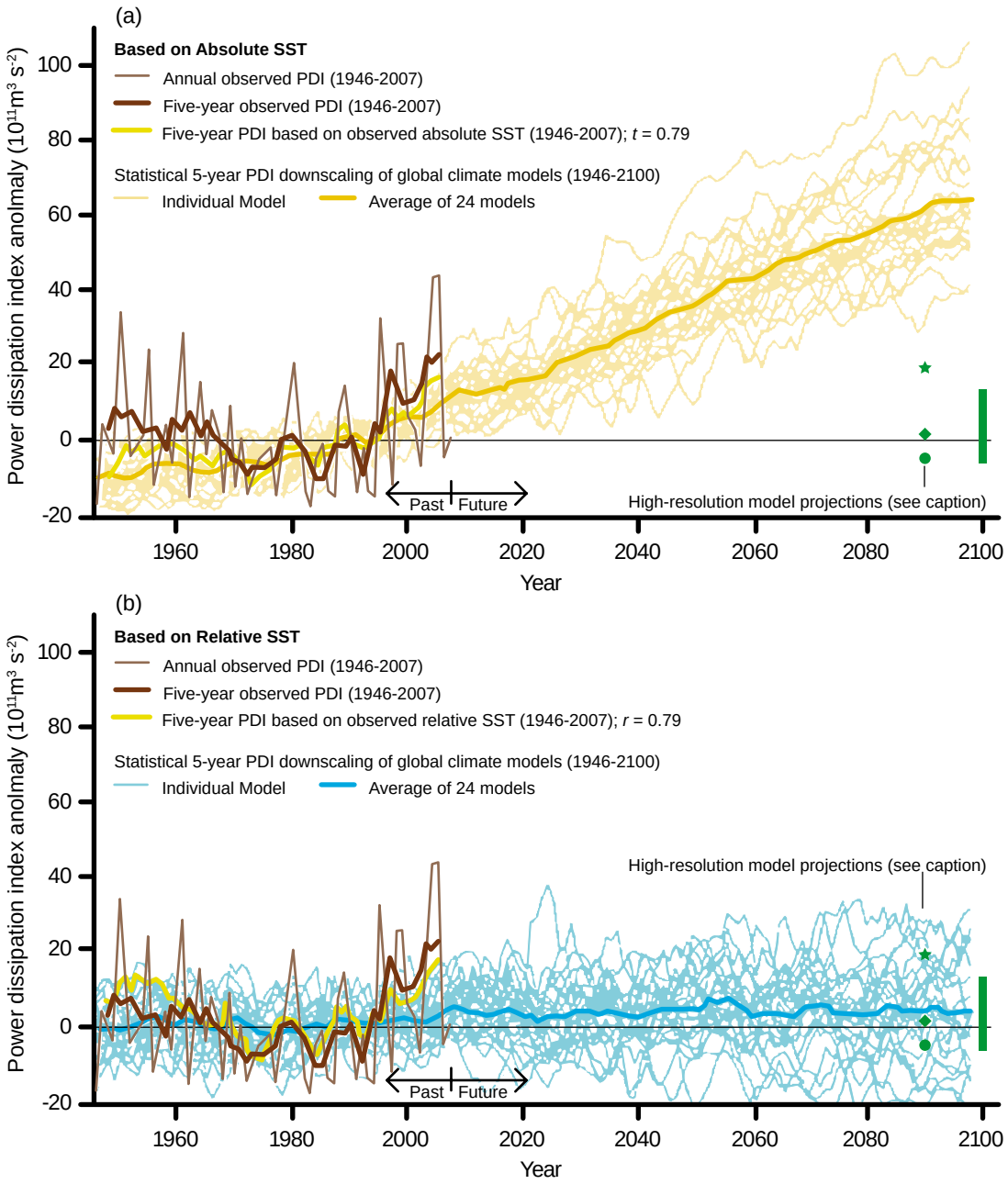

Observed PDI (Power Dissipation Index) anomalies are regressed onto observed absolute and relative SST (Sea Surface Temperature) over the period 1946 to 2007, and these regression models are used to build estimtes of PDI from output of global climate models for historical and future conditions. Anomalies are shown relative to the 1981 to 2000 average (2.13 x 10^{11} m^3s^{-2}). The green bar denotes the approximate range of PDI anomaly predicted by statistical/dynamical calculations. The other green symbols denote the approximate values suggested by high resolution dynamical models. SST indices are computed over the region 70°W-20°W, 7.5°N-22.5°N, and the zero-line indicates the average over the period from 1981 to 2000. (Source: Vecchi et al. 2008 and references therein)

An analysis of the observational record from south-east Australia for the period 1973–2007 shows that fire danger weather has increased by 10–40% in many areas for the period 2001–07 compared to the period 1980–2000 (Lucas et al. 2007). Climate model projections for continued warming and drying indicate a further increase of 5–65% in the incidence of such weather conditions by 2020 (Lucas et al. 2007). Simulations for the Australian Capital Territory using fire models show increased burnt area, a shorter interval between fires and an increase of 25% in fire intensity with a 2°C increase in mean annual temperature above pre-industrial levels (Cary 2002; Figure 27). An analysis that used climate scenarios for 2050 and 2100 (high and low emissions scenarios for each time) showed that the probability of extreme fire risk increased under all scenarios, dramatically so for the high emissions scenario for 2100 (Pitman et al. 2007).

Despite the complex relationship between climate change and fire regimes, the weight of evidence is clear. The risk of larger and more intense fires increases with increasing temperature, especially in those areas of the world, such as southern and eastern Australia, that are also experiencing drying trends (Cary et al. 2006).

Figure 27: Projected shift in the Australian Capital Territory bushfire regime.

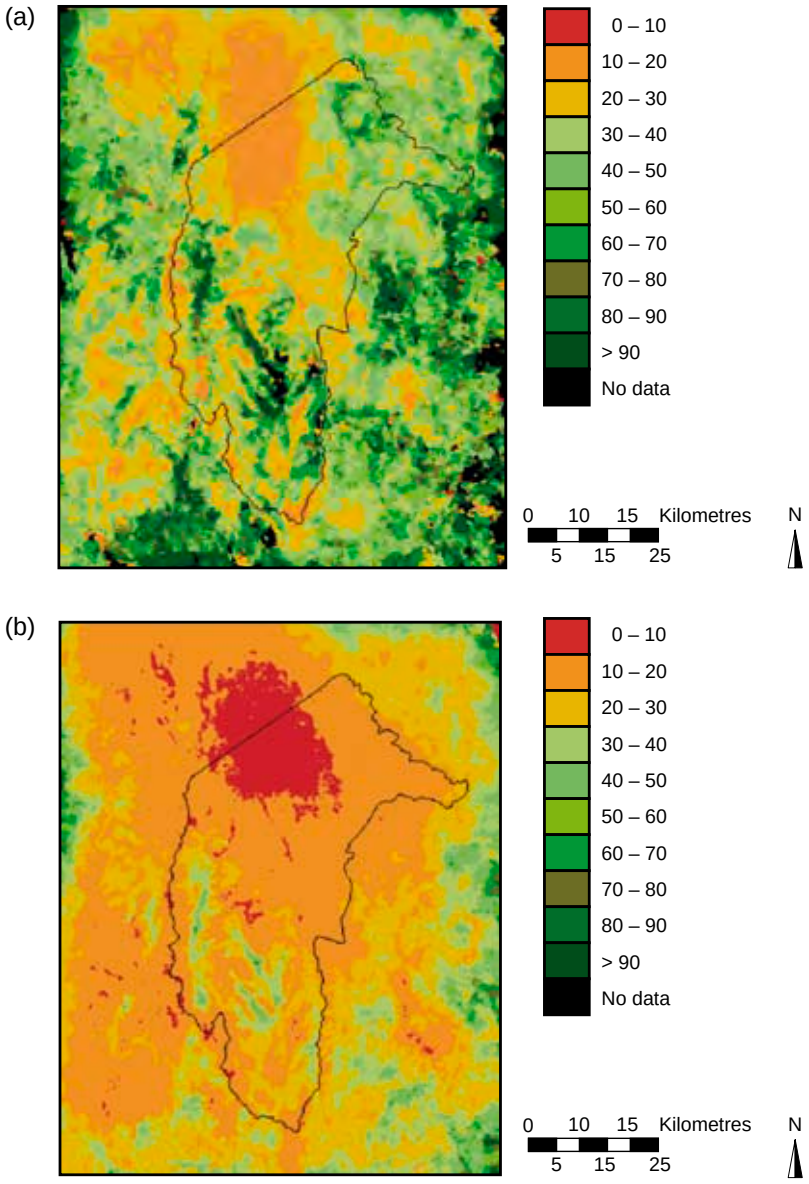

Average inter-fire interval for the Australian Capital Territory from a 500-year simulation with (a) current climate, and (b) moderate (mid-range IPCC projection) change in climate. (Source: Cary 2002)

2.5 Update on "reasons for concern"

The issues discussed in the previous sections – rising sea level, changing water resources, ocean acidification and extreme events – all have significant implications for human and societal well-being. The Third Assessment Report of the IPCC attempted to synthesise the information available at that time on these and other potential impacts of climate change on societies – the so-called "reasons for concern" or "burning embers" diagram. The results were presented as a relationship between potential impacts and increases in global mean temperature (Smith et al. 2001; Figure 28a).

Recently a team of researchers (Smith et al. 2009) carried out a preliminary update of the original IPCC reasons for concern, using the same methodology as before based on expert judgment. The new assessment draws on a large body of research over the past seven to eight years that has explored and refined the concept of vulnerability in the context of climate change. The results (Figure 28b) show that smaller increases in global mean temperature lead to significant potential impacts on human well-being, effectively lowering the temperature level for what might be considered dangerous climate change.

Figure 28. Risks from climate change by reason for concern (RFC) for 2001 compared with updated data.

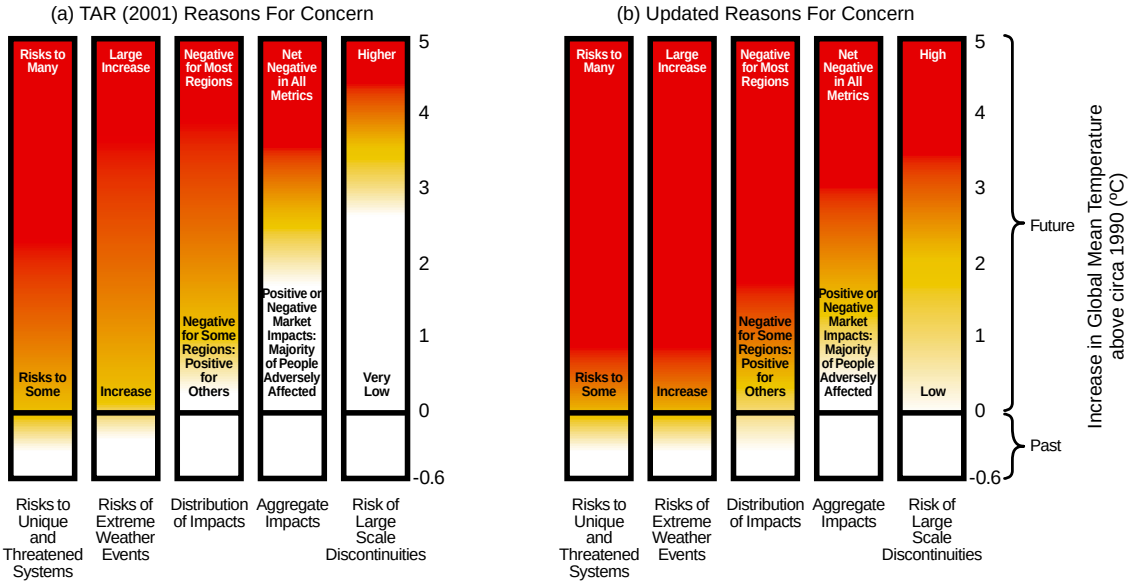

Climate change consequences are plotted against increases in global mean temperature (°C) after 1990. Each column corresponds to a specific RFC and represents additional outcomes associated with increasing global mean temperature. The colour scheme represents progressively increasing levels of risk. The historical period 1900 to 2000 warmed by ca. 0.6°C and led to some impacts. (A) RFCs from the IPCC Third Assessment Report as described in Smith et al. 2001. (B) Updated RFCs derived from IPCC AR4 as supported by the discussion in Smith et al. 2009.